

1 **Process-based three-layer synergistic optimal allocation**
2 **model for complex water resource systems considering**
3 **reclaimed water**

4 **Jing Liu¹ Yue-Ping Xu^{1*} Wei Zhang² Shiwu Wang³ Siwei Chen¹**

5 ¹ Institute of Water Science and Engineering, College of Civil Engineering and
6 Architecture, Zhejiang University, Hangzhou 310058, China

7 ² College of Computer Science and Technology, Zhejiang University, Hangzhou
8 310058, China

9 ³ Zhejiang Institute of Hydraulics & Estuary, Hangzhou 310020, China

10 *Corresponding author: Yue-Ping Xu, yuepingxu@zju.edu.cn

11 **Abstract**

12 The increasing water demand due to human activities has aggravated water scarcity,
13 and conflicts among stakeholders have increased the risk of unsustainable development.
14 Ignoring the effects of trade-offs leads to misguided policy recommendations. This
15 study highlights the concept of synergy among different aspects of water allocation
16 process. A process-based three-layer synergistic optimal allocation (PTSOA) model is
17 established to integrate the interests of stakeholders across sub-regions, decision levels
18 and time steps while simultaneously coupling reclaimed water to establish

19 environmentally friendly solutions. A synergy degree index is constructed by applying
20 network analysis for optimization. PTSOA is applied in Yiwu City, Southeast China,
21 and is shown to be able to improve the contradictions among different dimensionalities
22 in a complex system. Overall, $2.43 \times 10^7 \sim 3.95 \times 10^7$ m³ of conventional water is saved,
23 and notable improvements in management are achieved. The application demonstrates
24 the efficiency and excellent performance of the PTSOA model.

25 **Keywords** Three-layer optimization, water allocation, process, synergy, reclaimed
26 water

27 **1. Introduction**

28 Water scarcity has become one of the major impediments to sustainable development
29 of cities (Yue et al., 2020). Emerging water scarcity concerns in cities are associated
30 with limited available water, severe water pollution and relentlessly growing demand
31 for water as driven by industrial growth, population growth and higher living standards;
32 these factors have led to intense competition for freshwater among stakeholders of
33 interest (Dai et al., 2018; Wu et al., 2023). However, the heterogeneous distribution of
34 water resources at both spatial and temporal scales is common and results in water
35 shortage risks and conflicts, which often require the optimization of water resource
36 allocation (Friesen et al. 2017). Moreover, some satisfactory alternatives for individual
37 stakeholders may result in negative externalities on others. Nowadays, the water
38 resources system become more and more complex, and often has multiple sources and

39 users as well as water reused infrastructure. This kind of water resources system is
40 called complex system. Therefore, it is critical to develop a synergistic optimal
41 allocation model to alleviate conflicts and ensure the security, efficiency, equality, eco-
42 environmental sustainability, and sustainable development of complex water resources
43 systems simultaneously.

44 As equitable access to water resources is closely related to social stability, several
45 qualitative and indirect methods have been developed to assess water allocation
46 equality (D'Exelle et al. 2012). In cases with limited water resources, more water would
47 be allocated to users with better economic conditions to achieve more economic
48 benefits. Thus, stakeholders with poor economic status are ignored, resulting in
49 imbalanced development. Consequently, actions are often needed by local government
50 managers to avoid such situations. The Gini coefficient has been widely used to
51 evaluate equality and enhance the optimization of water allocation in water use sectors
52 (Xu et al. 2019; Hu et al. 2016; D'Exelle et al. 2012). However, it is unable to reflect
53 the dynamic interactions among objectives, i.e., how objectives interact with each other
54 and impact the equity of a system in cases with diverse alternative decisions. In the
55 perspective of coordinated allocation, multiple goals are simultaneously considered to
56 avoid negative effects as much as possible. Therefore, in addition to equity,
57 coordination should be considered in water allocation systems, and these two concepts
58 can be combined to promote systemic synergy. By identifying the dynamic interactions
59 among objectives, the internal mechanisms of a water system can be clarified, and

60 synergy can be achieved in cases with different potential decisions. It is also helpful to
61 identify the hurdles and opportunities associated with sustainable development for
62 cities and to establish specific action priorities for cities based on a comprehensive
63 understanding of the interactions among objectives. To address this knowledge gap, a
64 correlational network approach is applied in this study, and a synergy degree index is
65 presented to consider both equity and coordination of water systems. Moreover,
66 systemic analysis is used to assess the level of coordination of complex objective
67 interactions in city water systems.

68 Network analysis, which has been widely used in studies of complex systems (Ball
69 et al., 2000; Saavedra et al., 2011; Bond, 2017), is a holistic approach for exploring the
70 characteristics of interactions among objectives. It provides clear visualization and
71 conceptualization of the interactions among variables to fully characterize those
72 interactions (Swain and Ranganathan, 2021). An array of network metrics (for example,
73 degree centrality, betweenness centrality, eigenvector centrality, closeness centrality,
74 and community) can be applied to quantify the importance of objectives or targets in an
75 interaction network (Zhou and Moinuddin, 2017) and reveal the strongly connected
76 pairs of goals or targets in the network (Allen et al., 2019). A key network metric in
77 such analysis is connectivity, which reflects the degree of coordination among different
78 objectives in a system; in synergy networks, high connectivity indicates that many
79 objectives can be achieved simultaneously and that the negative effects of interactions
80 are mild (Wu et al., 2022). Thus, to facilitate the discovery of high-quality decision

81 alternatives, alleviate negative conflicts among multiple utilities and inform decision
82 making, a synergy degree evaluation index is established and applied to the network
83 analysis of this study.

84 Due to negative externalities of individual decisions, conflicts occur not only
85 across different users or objectives but also across hierarchical decision levels. Water
86 use contradictions and inconsistent decision making by multiple managers inevitably
87 results in trade-offs, including positive and negative water resource feedback in cases
88 with limited water availability (Wang et al., 2022). In practice, district administrators
89 allocate water to each sector in each sub-region, and sub-region managers then make
90 decisions based on the allocated amount of water resources (Safari et al., 2014). Since
91 each decision maker places emphasis on different targets, feedback and coordination
92 among different decision makers are of great importance. Therefore, synergistic
93 hierarchical water allocation that achieves coordination among different decision
94 makers is imperative to avoid conflicts, save water and maintain social stability.

95 To address these hierarchical problems, bi-level programming (BLP) has been
96 widely used, wherein objectives at two hierarchical levels, namely, an upper level and
97 a lower level, are co-optimized (Zhang and Vesselinov, 2016; Jin et al., 2018). The
98 upper-level decision may be affected by actions of the lower-level decision makers
99 (Arora and Gupta, 2009). Yue et al. (2020) formulated a bi-level programming (BLP)
100 framework to gain insight into the whole water allocation process with district
101 administrators and sub-regional farmers. Li et al. (2022) built a two-level model with

102 the overall interests of system managers at the top and the individual interests of water
103 supply departments at the bottom. The multi-level programming problem (MLPP) was
104 derived from the bi-level programming problem (BLPP) and is more applicable to real
105 world practices (Baky, 2014). However, limited studies have explored applying MLPP
106 (more than two levels) for water resource allocation, especially in cases with
107 unconventional water supplies.

108 To satisfy both long-term and short-term water needs and avoid unnecessary
109 administration costs and water resource use caused by lack of coordination among
110 different allocation steps, temporally synergistic allocation and optimization are needed
111 (Haguma and Leconte, 2018). In annual water resource planning, the monthly
112 variability of hydrologic regimes and non-stationarity of the daily water demand must
113 be considered. As an alternative example of synergistic allocation at different time steps,
114 Vicuna et al. (2010) used a monthly nonlinear programming model and an annual
115 sampling stochastic dynamic programming (SSDP) model to establish a monthly
116 operating policy. Haguma et al. (2015) proposed an optimization approach with two
117 separate time steps following the nested model approach. Haguma and Leconte (2018)
118 constructed deterministic and stochastic optimization models with two time steps (intra-
119 annual and inter-annual) and two levels of inflow variability: seasonal and inter-annual.
120 The purpose of their short-time-step model was to derive aggregate performance
121 functions associated with potential long-time-step decisions in these studies. However,
122 short-term benefits should not be overlooked due to their appreciable impact on long-

123 term effects. Accordingly, synergistic allocation that enhances both long-term and
124 short-term allocations is of great importance for water resource management in cities.
125 However, optimizing the structure of a model to achieve maximized benefits and
126 balancing the trade-offs among time steps are tasks that have rarely been studied. The
127 synergy among different time steps is addressed with a new innovative framework and
128 a corresponding algorithm in our study.

129 Most of the abovementioned traditional models are based on a benefit-oriented
130 mechanism, which leads to a high degree of satisfaction in high-benefit regions and
131 large water shortages in other regions. The existence of high-benefit regions in a city
132 during the allocation process often exacerbates regional disparities and heterogeneous
133 development. Moreover, spatial factors influence allocation results, especially when
134 there is spatial hierarchical heterogeneity among water resource allocation elements (Li
135 et al., 2022). It is thus appropriate to conceptualize water allocation problems in a
136 multistage framework that fully considers the interests of not only the regional authority
137 but also sub-regional managers (Yao et al., 2019). Hence, the synergy among sub-
138 regions must be considered to optimally allocate water resources. Ideally, the benefits
139 of all sub-regions should be integrated equally in the model, and the weights of hyper-
140 parameters should be adjusted to best support flexible policies.

141 The optimal allocation of conventional and unconventional water resources also
142 significantly impacts water security and aquatic ecosystems. The reuse of reclaimed
143 water is beneficial for alleviating high water supply pressure on conventional water

144 resources and reducing the emission of pollutants. To effectively integrate conventional
145 and unconventional water resources, Yang et al. (2008) and Han et al. (2008) introduced
146 unconventional water resources as critical factors in water management. Avni et al.
147 (2013) investigated the mixing of unconventional water resources with other
148 conventional water sources to meet the magnesium requirements for drinking water and
149 irrigation water. Yu et al. (2017) developed a cost–benefit analysis-based utilization
150 model for externally transferred water and desalinated water. The allocation of both
151 conventional and unconventional water has been widely studied, but there remains a
152 lack of methods to guide the synergistic allocation of conventional and unconventional
153 water resources and embed reclaimed water supply systems in allocation schemes. The
154 overexploitation of conventional water resources is not conducive to sustainable
155 development, while extensive use of unconventional water could ultimately result in
156 high economic burden. To synergistically integrate conventional and unconventional
157 water resources and guide the coordinated allocation of these two types of water
158 resources, corresponding mechanisms must be implemented. As a result, our study aims
159 to couple the allocation of conventional water resources and unconventional water
160 resources to establish synergistic solutions.

161 In summary, as insufficient water supplies and increasing water demands intensify
162 competition for water resources and lead to conflicts among different stakeholders in
163 different dimensions, water allocation must be optimized in cities and regions to
164 achieve synergistic decision-making at various levels and time steps considering the

165 value of reclaimed water. Therefore, a new process-based three-layer synergistic
166 optimal allocation (PTSOA) model is developed here to generate numerous candidates
167 or Pareto solutions and identify several desirable decision alternatives. The synergy of
168 time and space optimization is achieved in the new model to avoid waste and promote
169 balanced spatial development. Furthermore, in the PTSOA model, reclaimed water is
170 used to replenish conventional water resources in water-scarce areas.

171 The remainder of this paper is organized as follows. The mathematical model is
172 formulated in Section 2. Section 3 gives a numerical example for Yiwu city to
173 demonstrate the effectiveness and efficiency of the proposed methods. The results are
174 shown in Section 4; different water allocation strategies under varying inflow
175 conditions are explored, and policy implications are discussed. Section 5 presents
176 conclusions.

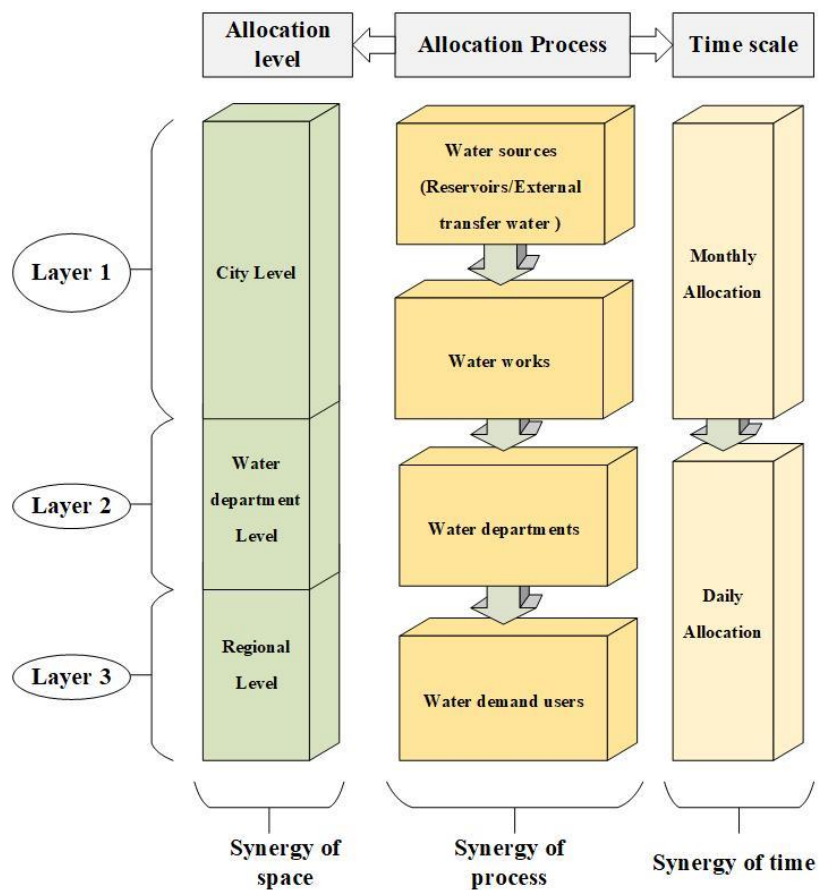
177 **2. Modelling**

178 With water resources becoming increasingly scarce, multi-dimensional synergistic
179 optimal allocation in a hierarchical system is crucial for ensuring sustainable
180 development in water-scarce cities. There are three dimensions of synergy in the
181 established allocation model, as shown in Fig. 1: process synergy, decision-level
182 synergy and time-scale synergy. The synergy of the process refers to synergistic water
183 allocation among the three stages throughout the whole allocation process to reduce
184 waste in bridging processes, which has rarely been considered. In the three stages, first,

185 the original water is released from reservoirs or diverted from external water transfer
186 projects to water works; then, the water stored in water works infrastructure is supplied
187 to different departments that need different types of water, including both conventional
188 and reclaimed water. Finally, water is supplied to different users. Decision-level
189 synergy refers to synergistic water allocation considering the interests of decision
190 makers at different levels, namely, the city, water department and regional levels, to
191 coordinate solutions and avoid conflicts among decision makers. The city level
192 represents the overall interests of a city from the perspective of government, the water
193 supply department level represents the interests of water supply corporations, and the
194 regional level focuses on the comprehensive benefits of each region in the city and
195 mitigate development imbalance among regions. Optimal decision making at the
196 department level is constrained by the allocation results at the city level, and so on, and
197 the final solution should satisfy the needs of decision makers across all levels. The time
198 scale synergy involves the coordination of the daily configuration goal with the monthly
199 goal, the monthly goal with the yearly goal, and so on. Synergistic temporal allocation
200 can largely alleviate time conflicts during configuration operations, ensuring that all
201 configuration periods serve the same final configuration objectives to save water
202 resources and improve efficiency. However, time scale synergy mainly depends on
203 artificial operations rather than automated intelligent operations in practice. In-depth
204 exploration has yet to be demonstrated. Consequently, the PTSOA model is constructed
205 here to fully consider these three dimensionalities of synergy. The dimensionalities are

206 coupled in this model to achieve the efficient maximization of comprehensive benefits
 207 at all levels under the premise of saving water resources. In Fig. 1, the grey boxes
 208 indicate the three different allocation dimensions, the green boxes indicate the three
 209 different decision levels coupled with spatial scales, the bright yellow boxes indicate
 210 every key nodes in the whole allocation process and the buff boxes indicate nested time
 211 scale.

212



213

214

Fig. 1. Conceptual map of the PTSOA model

215

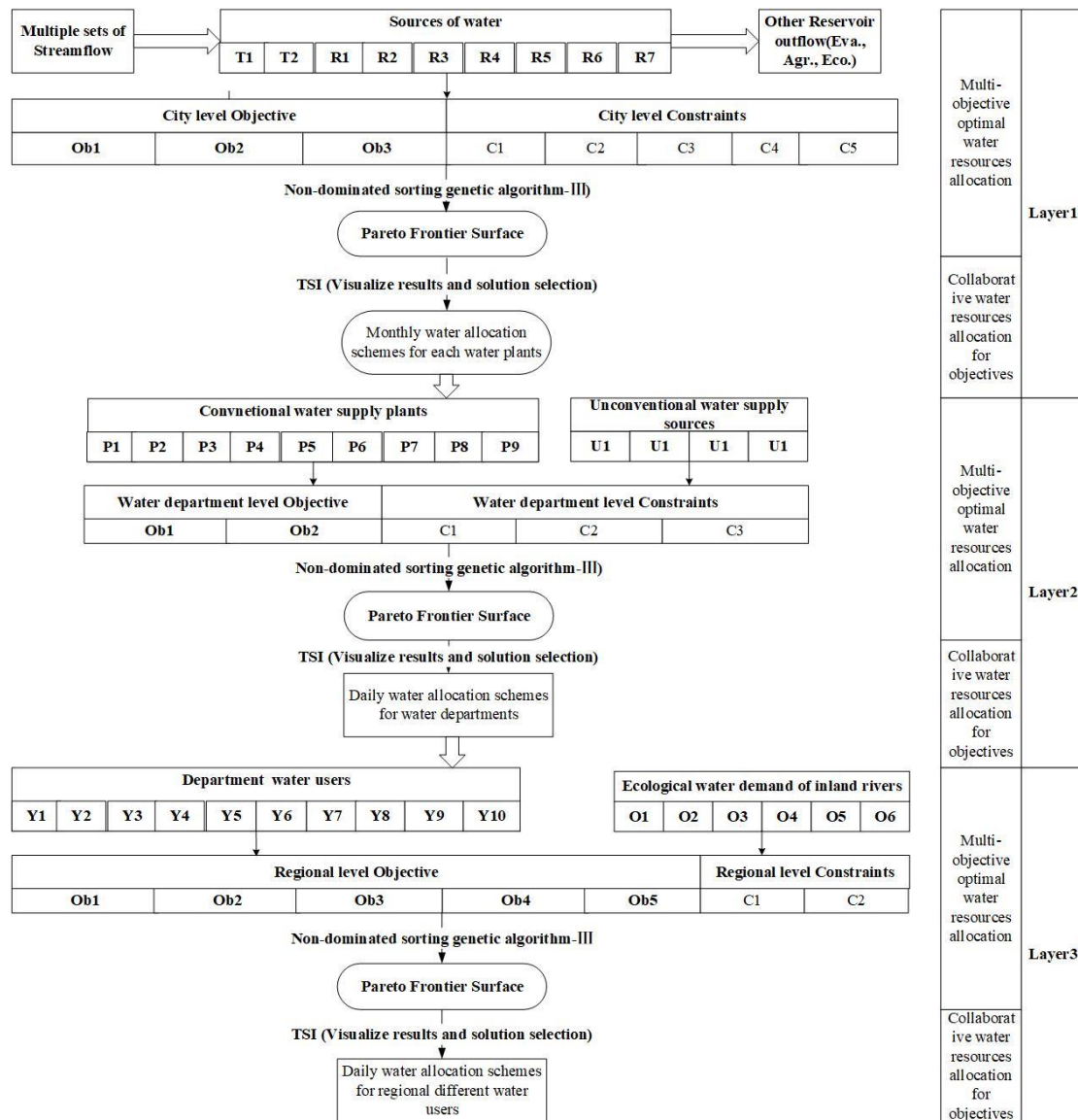
216 In water-scarce cities, using reclaimed water as an alternative water source is

217 proved to be useful to efficiently improve the environment by reducing sewage
218 discharge. The quality of inland tributaries has deteriorated in many water-scarce cities
219 due to limited consideration of the water environment and the large-scale emission of
220 pollutants. Transferring reclaimed water and main river water to urban inland tributaries
221 for ecological water replenishment is a promising approach for improving the quality
222 of urban water environments and areas with water shortages. However, there has been
223 a lack of studies on the integration of reclaimed water reuse systems and inland water
224 distribution systems in allocation modelling. Therefore, in addition to saving water
225 resources and improving efficiency through multi-dimensional synergistic allocation,
226 the model encompasses reclaimed water reuse systems and ecological water
227 distribution systems for inland tributaries.

228 Finally, the PTSOA model is constructed to solve the multi-dimensional synergistic
229 allocation problem involving complex water resource networks that couple reclaimed
230 water reuse systems and inland ecological water distribution systems with multiple
231 sources, processes and regions to guarantee the sustainable development of water-
232 scarce cities. To select the most synergistic solution of the PTSOA model, a new
233 evaluation index named the synergy index (*TSI*) is proposed to assess the synergy
234 degree of different decision alternatives. System entropy ($H(S)$) can describe the
235 evolution direction of a water resource system and was used to promote the
236 coordination of water supply departments in a water resource allocation system(Li et
237 al., 2022). So, it is used for comparison to evaluate the validity of this proposed index.

238 Furthermore, the network analysis method is applied for the first time to analyse
239 dynamic interactions in water optimal allocation. This method visually depicts the
240 dynamic interactions and conflicts among different subareas in a city, which is helpful
241 for system managers to realize how the water allocation scheme in one region
242 influences that of other areas; consequently, more reasonable and flexible measures are
243 established based on dynamic regional development targets. The detailed framework
244 developed in this study is shown in Fig. 2. In this figure, there are three layers in the
245 framework and each layer has two parts: multi-objective optimal water resources
246 allocation and collaborative water resources allocation for objectives. In the multi-
247 objective optimal water resources allocation, sub-layers contain key nodes in the
248 allocation process and relevant objectives and constraints. In the collaborative water
249 resources allocation for objectives, sub-layers contain optimization algorithm and
250 decision selection method.

251



252

253

Fig. 2. Framework of the PTSOA model

254 **2.1 First layer of the PTSOA decision-making process**

255 Three dimensionalities of synergistic water resource allocation are coupled in the first

256 layer of the PTSOA model. The first stage of the process (original water is released

257 from reservoirs or external water transfer projects to water works) is optimized in the

258 first layer. This stage demonstrates a strong constraint effect on the later stages. To

259 satisfy the overall development goals of the city, the first-layer processes involve city-
 260 level decision-making. The city manager focuses on the overall goal of the complex
 261 water resources system in the city, which is the first and most important phase of the
 262 decision-making process. The established allocation scheme highly influences decision
 263 makers at other levels, and optimal allocation schemes at other levels must align with
 264 this overall goal. Additionally, since water resource planning in most Chinese cities is
 265 based on an annual planning period and monthly planning unit, the time step of the first
 266 layer is set as months. Finally, the monthly decision alternatives for the volume of water
 267 allocated from reservoirs to water works is obtained at the city decision level.

268 **2.1.1 Objective functions of the first layer**

269 **Social objective function: minimization of total water supply shortages**

270 The social objective function is established by the city manager to minimize the total
 271 water supply shortages in a water system. The objective is established to sufficiently
 272 meet the water demands of users in a water resources system. The water deficit is
 273 considered, and this objective can reflect the ability of the water supply to meet the
 274 water demand, as shown in Eqs. (1-3):

$$275 \quad \min f_{11}(x) = D - S \quad (1)$$

$$276 \quad D = \sum_{r=1}^R \sum_{t=1}^T D_r^t \quad (2)$$

$$277 \quad S = \sum_{t=1}^T \sum_{i=1}^I \sum_{j=1}^J x_{ij}^t \alpha_{ij} + \sum_{t=1}^T \sum_{e=1}^E \sum_{j=1}^J x_{ej}^t \beta_{ej} \quad (3)$$

278 where $D (10^4 \text{ m}^3)$ is the total water demand of the system, $D'_r (10^4 \text{ m}^3)$ is the water
279 demand of the r th sub-region at t th time step, $r= 1,2, \dots, R$, R is the total number of sub-
280 regions in the area, $t=1,2, \dots, T$, T is the total number of months in the period, $S (10^4 \text{ m}^3)$
281 is the total water supply of the water system for all waterworks, $x'_{ij} (10^4 \text{ m}^3)$ is the
282 amount of water supplied from i th reservoir to the j th waterworks in the t th month of
283 the configuration period, $i=1,2, \dots, I$, I refers to the total number of reservoirs, $j=1,2, \dots, J$,
284 J is the number of total water works, $x'_{ej} (10^4 \text{ m}^3)$ is the amount of water supplied from
285 the e th external transfer water source to the j th water works in the t th month of the
286 configuration period, $e=1,2, \dots, E$, E is the total number of external transfer water
287 sources in the city, α_{ij} is the water supply relationship coefficient between the i th
288 reservoir and the j th water works, where 0 indicates no supply and 1 indicates a water
289 supply, and β_{ej} is the water supply relationship coefficient between the e th external
290 transfer water source and the j th water works, where 0 indicates no supply and 1
291 indicates a water supply.

292 **Economic objective function: maximization of the total water supply benefit**

293 A city manager operates a water allocation system to maximize the overall economic
294 benefit by establishing an economic objective function, as shown in Eqs. (4-7):

295
$$\max f_{12}(x) = B - C_{rs} - C_{es} \quad (4)$$

296
$$C_{rs} = k \times \sum_{t=1}^T \sum_{i=1}^I \sum_{j=1}^J x'_{ij} \alpha_{ij} + \sum_{t=1}^T \sum_{i=1}^I \sum_{j=1}^J (x'_{ij} \alpha_{ij} \times c_i) \quad (5)$$

297
$$C_{es} = m \times \sum_{t=1}^T \sum_{j=1}^J \sum_{e=1}^E x'_{ej} \beta_{ej} + \sum_{t=1}^T \sum_{e=1}^E \left(n_e \times \sum_{j=1}^J x'_{ej} \beta_{ej} \right) \quad (6)$$

$$B = \sum_{j=1}^J b_j \times \left(\sum_{t=1}^T \sum_{i=1}^I x_{ij}^t \alpha_{ij} + \sum_{t=1}^T \sum_{e=1}^E x_{ej}^t \beta_{ej} \right) \quad (7)$$

299 The overall economic benefit is the difference between the total benefit and total
300 cost at the city level. In the equations, B (Chinese Yuan is the total direct water supply
301 benefit (mainly considering the income from water charges for the city). The total water
302 supply cost consists of the reservoir water supply cost C_{rs} and the external water
303 supply cost C_{es} ; k (Chinese Yuan/m³) denotes the water resources fees paid to the
304 government; c_i (Chinese Yuan/m³) denotes the water fees paid to the i th reservoir
305 authority; m (Chinese Yuan/m³) is the charge to an external administrative district per
306 unit of externally transferred water; n_e (Chinese Yuan/m³) is the charge associated with
307 the e th external water source per unit of transferred water; and b_j (Chinese Yuan/m³)
308 is the unit price of water supply revenue for the j th user.

309 **Sustainable development objective function: maximization of the total amount of**
310 **reserved water in reservoirs**

311 In water-scarce cities, the problem of water scarcity is a serious challenge that prevents
312 sustainable allocation of water resources. A prominent feature of most water-scarce
313 cities is that water inflows are limited, and the fluctuations in water availability are
314 large. Therefore, to reduce the risk that the inflows in the next configuration period are
315 too short to meet the basic demand of the city, a sustainable development objective
316 function is developed. The sustainable development objective function seeks to
317 maximize the amount of water remaining in the reservoir at the end of a configuration

318 period to hedge against drought risk and guarantee water use in the next period, as
 319 shown in Eqs. (8-10):

$$320 \quad \max f_{13}(x) = \sum_{i=1}^N (V_i^{\max} - V_i) \times p(V_i^{\max} - V_i) \quad (8)$$

$$321 \quad p(V_i^{\max} - V_i) = \begin{cases} 2 \times V_i / V_i^{\max} & 0 < V_i < V_i^{\max} / 2 \\ -2 \times V_i / V_i^{\max} + 2 & V_i \geq V_i^{\max} / 2 \end{cases} \quad (9)$$

$$322 \quad V_i = \sum_{t=1}^T (R_{i,initial} + I_i^t + P_i^t - A_i^t - E_i^t - EP_i^t) - \sum_{t=1}^T \sum_{j=1}^J x_{ij}^t \alpha_{ij} \quad (10)$$

323 where V_i^{\max} (10^4 m^3) is the maximum allowable storage capacity of the i th water source,
 324 which is expressed based on the limited storage capacity of a reservoir in the flood
 325 season, and V_i (10^4 m^3) is the water storage capacity of the i th water source at the end
 326 of the scheduling period. As much water as possible but less than V_i^{\max} is reserved.
 327 However, a reserved water volume in the reservoir that is too high at the end of the
 328 scheduling period may lead to considerable pressure on reservoirs to urgently release
 329 water if a flood event is forecasted. The reserved water volume should be neither too
 330 large nor too small. Thus, the benefits of reservoir reserve stock must be thoroughly
 331 evaluated. Based on the characteristic of the benefit of residual water, we propose a
 332 boundary benefit function $p(V_i^{\max} - V_i)$ for different reserved water volumes in a
 333 reservoir. The benefit function is a piecewise function, and when V_i is less than
 334 $V_i^{\max} / 2$, p increases as V_i increases. When V_i is equal to or greater than $V_i^{\max} / 2$, p
 335 decreases as V_i increases. When $V_i = V_i^{\max}$, p decreases to 0. $R_{i,initial}$ (10^4 m^3) is the
 336 initial storage of the i th water source, I_i^t (10^4 m^3) is the inflow of the i th water source

337 at the t th time step, P_i^t (10^4 m^3) is the precipitation associated with the i th water source
 338 at the t th time step, A_i^t (10^4 m^3) and E_i^t (10^4 m^3) are the agricultural and ecological
 339 water supplies associated with the i th water source at the t th time step, respectively, and
 340 EP_i^t (10^4 m^3) is the evaporation from the i th water source at the t th time step.

341 **2.1.2 Constraints of the first layer**

342 The layer includes six main constraints: the reservoir water supply constraint, water
 343 demand constraint, reservoir storage constraint, water balance constraint, external water
 344 transfer constraint, and nonnegative constraint.

345 **Reservoir water supply constraint**

346 The maximum water available to supply from an individual reservoir is determined by
 347 the difference between the total input and total reservoir output. The inputs include
 348 inflow and precipitation, and the outputs mainly involve agricultural and environmental
 349 water supplies, evaporation, water supplied for waterworks and reservoir leakage loss.

350 All these factors directly affect the decision-making process and are incorporated into
 351 the model building process as shown in Eqs. (11-15):

$$352 \quad V_i^t \leq V_{i,\max}^t \quad (11)$$

$$353 \quad V_i^t = \sum_{j=1}^J x_{ij}^t \alpha_{ij} \quad (12)$$

$$354 \quad V_{i,\max}^t = \sum_{l=1}^{t-1} \left(R_{i,\text{initial}} + I_i^l + P_i^l - A_i^l - E_i^l - EP_i^l - \sum_{j=1}^J x_{ij}^l \alpha_{ij} - L_i^l \right) - V_{i,d} \quad (13)$$

$$355 \quad EP_i^t = ep_i^t \times s_i^t / 1000 \quad (14)$$

356
$$V_i^t = \xi_i^t \times (R_i^{t-1} + R_i^t) \quad (15)$$

357 where V_i^t (10^4 m^3) denotes the total water supply from the i th reservoir at the t th time
 358 step; $V_{i,\max}^t$ (10^4 m^3) is the maximum water available to be supplied from the i th
 359 reservoir at the t th time step; ep_i^t (mm) is the water surface evaporation from the i th
 360 reservoir in the t th month; s_i^t (m^2) is the monthly average surface area of the i th
 361 reservoir in the t th month; $V_{i,d}$ (10^4 m^3) is the dead storage of the i th reservoir; L_i^t (10^4
 362 m^3) is the reservoir leakage loss from the i th reservoir at the t th time step; R_i^{t-1} (10^4 m^3)
 363 is the storage of the i th reservoir at the $t-1$ th time step; R_i^t (10^4 m^3) is the storage of the
 364 i th reservoir at the t th time step; and ξ_i^t is the t th monthly leakage coefficient for the
 365 i th reservoir.

366 **Water demand constraint**

367 The high-quality water demand of each subarea in a city should be satisfied in the water
 368 allocation process. High-quality water in this model refers to water that satisfies the
 369 relevant primary (surface water can be used for drinking after simple purification
 370 treatment, such as filtration and disinfection) and secondary water quality requirements
 371 (water is slightly polluted and can be used for drinking after routine purification
 372 treatment, such as flocculation, precipitation, filtration, disinfection, and other
 373 processes) according to the Chinese Standard (GB5749), as shown in Eq. (16):

374

375
$$0.8 \times D_r \leq \sum_{t=1}^T \sum_{i=1}^I \sum_{j=1}^{J_r} x_{ij}^t \alpha_{ij} + \sum_{t=1}^T \sum_{e=1}^E \sum_{j=1}^{J_r} x_{ej}^t \beta_{ej} \leq 1.2 \times D_r, r = 1, 2, \dots, R \quad (16)$$

376 where D_r (10^4 m^3) is the high-quality water demand in the r th sub-region and there
 377 are a total of R sub-regions in the city. J_r is the number of waterworks in the r th sub-
 378 region. To ensure that the water supply guarantee in each area is greater than 80%, the
 379 total water supplied to every subarea is greater than 80% of its demand.

380 **Reservoir storage constraint**

381
$$R_i^T \leq V_{i,f} \quad (17)$$

382
$$R_i^T = \sum_{t=1}^T \left(R_{i,initial} + I_i^t + P_i^t - A_i^t - E_i^t - EP_i^{t1} - \sum_{j=1}^J x_{ij}^t \alpha_{ij} - V_i^t \right) \quad (18)$$

383 where R_i^T (10^4 m^3) is the storage of the i th reservoir at the end of the configuration
 384 period and $V_{i,f}$ (10^4 m^3) is the flood-limit storage capacity.

385 **Water balance constraint**

386
$$R_i^{t+1} = R_i^t + I_i^t + P_i^t - A_i^t - EP_i^t - E_i^t - V_i^{t-1} - \sum_{j=1}^J x_{ij}^t \quad (19)$$

387 **External transfer water constraint**

388
$$\sum_{t=1}^T \sum_{j=1}^J x_{ej}^t \beta_{ej} \leq E_{e,max} \quad (20)$$

389 where $E_{e,max}$ refers to the maximum water supply capacity of *an* external water source
 390 over the whole configuration period.

391 **Nonnegative constraint**

392
$$x_{ij} \geq 0 \quad (21)$$

393 **2.2 Second layer of the PTSOA decision-making model**

394 Similarly, the second layer of the PTSOA model fuses all three dimensions of
395 synergistic water resource allocation mentioned previously. The second stage of the
396 process (the water stored in water works is supplied to different departments needing
397 water volumes of different quality) is optimized in the second layer. After city-level
398 decision-making, a conflict of interest inevitably occurs between traditional water
399 supply departments and unconventional water supply departments. Because
400 conventional and unconventional water supply departments compete for limited water
401 demand market shares, the stability of the water allocation system may be jeopardized
402 if excessive competition is not controlled. Thus, the second layer is implemented at the
403 department level. Decision-making at the department level seeks to guide the two water
404 supply departments to partake in benign competition and avoid conflicts to realize
405 synergy. In this case, the decision plan of the first layer in the hierarchy is followed.
406 Temporally, short-term allocation changes are needed as mentioned above; hence, the
407 time scale of the second layer is daily. Thus, the daily decision alternatives for the
408 volume of water allocated from water works to different water departments are obtained
409 to make relevant decisions.

410 **2.2.1 Objective functions of the second layer**

411 **Conventional water supply department objective function: minimization of the**

412 **total amount of water retained in water works**

413 The managers of conventional water supply departments strive to operate conventional
414 water systems efficiently and achieve the most equitable water share possible. The
415 amount of conventional water (of high quality) retained in a water works system is a
416 crucial factor affecting the efficiency and benefits of conventional water supply
417 departments. Therefore, the benefit of conventional water departments is established by
418 minimizing the total amount of water retained in water works at the end of a
419 configuration period, as shown in Eq. (22):

420
$$\min f_{21}(x) = W_L = \sum_{t=1}^T \sum_{i=1}^I \sum_{j=1}^J x_{ij}^t \alpha_{ij} + \sum_{t=1}^T \sum_{e=1}^E \sum_{j=1}^J x_{ej}^t \beta_{ej} - \sum_{t=1}^T \sum_{m=1}^M \sum_{j=1}^J \sum_{z=1}^Z q_{jz}^{t,m} \chi_{jz} \quad (22)$$

421 where W_L (10^4 m³) is the total amount of water retained in a water works system at
422 the end of a configuration period; $q_{jz}^{t,m}$ (10^4 m³) is the water supply from the j th water
423 works system to the z th water user on the m th day in the t th month in the period of
424 configuration; $m=1,2,\dots,M$; and M is the total number of days in the t th month (28, 29,
425 30 or 31). Additionally, $z=1,2,\dots,Z$, and Z is the total number of water users. χ_{jz} is the
426 water supply relationship coefficient between the j th water work and the z th water user,
427 where 0 indicates no supply and 1 indicates water supply.

428 **Unconventional water supply objective function: maximization of the amount of**
429 **unconventional water supplied**

430 The reclaimed water reuse system and ecological water distribution system for inland
431 tributaries are incorporated into the PTSOA model which are associated with

432 unconventional water supply departments. The managers of unconventional water
 433 supply departments seek to supply as much unconventional water as possible to
 434 promote their interests. Thus, the objective of unconventional water departments is
 435 established to maximize the amount of unconventional water supplied. Unconventional
 436 water mainly includes reclaimed water and river water, which is of low quality (i.e., not
 437 meeting the quality standard mentioned in Section 2.1.2) and is mainly used for
 438 industrial production, ecological water replenishment for inland rivers and municipal
 439 road sprinkling.

440 Unconventional water departments operate reclaimed water reuse systems and
 441 ecological water distribution systems to supply unconventional water, and the
 442 associated equations are as follows in Eqs. (23-26):

$$443 \quad \max f_{22}(x) = W_r + EW_r \quad (23)$$

$$444 \quad W_r = \sum_{t=1}^T \sum_{n=1}^N \sum_{j=1}^J r_{nj}^t p(b_c, b_u) \theta_{nj} \quad (24)$$

$$445 \quad p(b_c, b_u) = \frac{1}{3} \times \frac{b_c}{b_u} - \frac{2}{3} \quad (25)$$

$$446 \quad EW_r = \sum_{t=1}^T \sum_{n=1}^N \sum_{z=1}^Z r_{nz} \theta_{nz} \quad (26)$$

447 where W_r (10^4 m^3) is the total amount of reclaimed water supplied for all water users;
 448 EW_r (10^4 m^3) is the total amount of river water supplied to maintain ecological flows
 449 in inland tributaries; r_{nj}^t (10^4 m^3) is the amount of water supplied to the j th user from
 450 the n th reclaimed water source at the t th time step; $n = 1, \dots, N$; N is the total number of

451 reclaimed water sources; $p(b_c, b_u)$ is a function expressing the willingness of residents
 452 to use reclaimed water, b_c (Chinese Yuan/ 10^4 m³) is the price per unit of conventional
 453 water; b_u (Chinese Yuan/ 10^4 m³) is the price per unit of unconventional water; and θ_{nj}
 454 is the water supply relationship between the n th reclaimed water source and the j th user.
 455 In this case, $\theta_{nj} = 1$ indicates a water supply relationship, and $\theta_{nj} = 0$ indicates no
 456 water supply relationship. r_{nz} (10^4 m³) is the amount of water supplied from the n th
 457 reclaimed water source to the z th inland tributary; $z = 1, 2, \dots, Z$; Z is the total number of
 458 inland tributaries requiring ecological flow compensation; and θ_{nz} is the water supply
 459 relationship between the n th reclaimed water source and the z th inland tributary.

460 2.2.2 Constraints of the second layer

461 Conventional water supply constraint

462 According to conservation of mass, the total daily amount of conventional water
 463 allocated in the second layer should be less than the total monthly amount of
 464 conventional water allocated in the first layer, as described in Eq. (27):

$$465 \quad \sum_{t=1}^T \sum_{i=1}^I \sum_{j=1}^J x_{ij}^t \alpha_{ij} + \sum_{t=1}^T \sum_{e=1}^E \sum_{j=1}^J x_{ej}^t \beta_{ej} \geq \sum_{t=1}^T \sum_{m=1}^M \sum_{j=1}^J \sum_{z=1}^Z q_{jz}^{t,m} \chi_{jz}, t = 1, \dots, T \quad (27)$$

466 Unconventional water constraints

467 The two types of unconventional water have separate constraints. For reclaimed water
 468 supplied to water users, the amount should satisfy the relevant water recycling standard.
 469 The ecological water used to replenish inland tributaries is mainly pumped from

470 reclaimed water works and main rivers. Therefore, this replenished volume is limited
 471 by the pumping capacity. The constraints for unconventional water are shown in Eqs.
 472 (28)-(29):

$$473 \quad \sum_{t=1}^T \sum_{n=1}^N \sum_{j=1}^J r_{nj}^t \theta_{nj} + \sum_{t=1}^T \sum_{n=1}^N \sum_{z=1}^Z r_{nz}^t \theta_{nz} = \sum_{t=1}^T \sum_{i=1}^I \sum_{j=1}^J x_{ij}^t \delta_{ij} \eta_{ij} + PU \quad (28)$$

$$474 \quad PU = \sum_{t=1}^T \sum_{m=1}^M \sum_{p=1}^P Q_{t,m}^{p,s} / 10^4 \quad (29)$$

475 where δ_{ij} is the sewage discharge coefficient, which is the proportion of the water
 476 supplied from sewage discharge; η_{ij} is the sewage water reuse rate, which is the
 477 proportion of reused water in the total volume of sewage water; PU (10^4 m³) is the
 478 amount of water pumped from the main river; and $Q_{t,m}^{p,s}$ (t/d) is the flow through the
 479 sth pumping station on the mth day at time step t .

480 **Pumping constraints**

$$481 \quad Q_{t,s}^p \leq Q_{\max,s}^p \quad (30)$$

$$482 \quad Q_t^p = \sum_{s=1}^{Np} r_{t,s}^p \quad (31)$$

483 where $Q_{\max,s}^p$ (t/d) denotes the upper flow boundary of the sth pumping station; r_t^s (t/d)
 484 is the power of the p th pump installed at the sth pump station; and Np is the number of
 485 pumps stalled at the sth pump station.

486 **Water quality constraint**

487 To control the impacts of various point and nonpoint sources on receiving water bodies
 488 in cities, water authorities impose water quality standards for the management of river

489 basins. These standards seek to maintain the water quality at a desired target level by
 490 defining discharge limits for conventional, specific, or priority pollutants. To satisfy the
 491 relevant standards, the following water quality constraint is established:

$$492 \quad \sum_{t=1}^T \sum_{i=1}^N \sum_{j=1}^M \left(x_{ij}^t \delta_{ij} \psi_{ij} h_j^u - x_{ij}^t \delta_{ij} \eta_{ij} h_j^u \right) \times 10 \leq H^u \quad (32)$$

493 where ψ_{ij} is the sewage water treatment rate, which is the proportion of sewage water
 494 that is treated; h_j^u (mg/L) is the concentration of the u th contaminant per unit treated
 495 water required by the j th user; and H^u (kg) is the upper limit of the u th contaminant
 496 allowed to be discharged in the study area.

497 **2.3 Third layer of the PTSOA decision-making model**

498 After obtaining the results for the former two stages of the allocation process and the
 499 two levels of decision-making, the third model layer is constructed to achieve regional
 500 synergy. It refers to the collaborative allocation of water resources in different sub-
 501 regions of a city, and it is intended to balance and maximize the interests of each sub-
 502 region as much as possible. Additionally, the needs of different kinds of water users in
 503 different sub-regions can be met to the greatest extent possible with this approach.
 504 Therefore, the three dimensions of synergy are also fused in this layer. The third stage
 505 of the process (the water in different departments is supplied to different kinds of water
 506 users, namely, residential users, industrial users and municipal users, in different sub-
 507 regions) is optimized in this layer. After department-level decision-making, conflicts of

508 interest inevitably occur among various water users in different sub-regions of a city.
509 Therefore, the third layer considers regional-level decision-making to coordinate water
510 needs and avoid conflicts of sub-regions in the city. Moreover, the various development
511 priorities of sub-regions are emphasized by adjusting certain hyper-parameters in the
512 third layer. This layer is established based on the allocation scheme obtained in the
513 second layer of the hierarchy, and the time scale of this layer is the same as that of the
514 second.

515 Although water pollutants are controlled in the second layer, the detailed spatial
516 distribution of pollutants remains unknown. If one of the sub-regions emits a greater
517 pollution load than others such that the river pollution limit is exceeded, it constrains
518 sustainable development and undermines the fairness of the allocation. To ensure the
519 coordination of water quality among regions, the representative pollutant concentration
520 of the main reach in each sub-region after configuration should meet the relevant
521 environmental capacity requirements. If these requirements are not met, the objective
522 function for this sub-region will call for a punishment, and more environmentally
523 friendly plans will be searched. After sewage with pollutants is transported from outlets
524 to water bodies, advective transport, longitudinal dispersion and transverse mixing will
525 occur. At the same time, physical, chemical and biological interactions will occur in the
526 water body. To objectively describe the degradation of pollutants in water, it is
527 necessary to use mathematical models to simulate physical dynamics. Due to the
528 heterogeneity of pollutants entering water bodies and the uncertainty of hydrological

529 processes, it is usually of little practical significance to calculate the change in river
 530 water capacity over time. A steady-state model is therefore used to calculate the water
 531 capacity of the target water body (Cetintas et al., 2010; Zhang et al., 2019). When water
 532 quality changes are studied at the annual scale and complete mixing is assumed, the
 533 following equation can be used to describe the water quality change, as shown in Eq.
 534 (33):

$$535 \quad \frac{Vdc}{dt} = Q(Ce - C) + Sc + r(c)V \quad (33)$$

536 where V (m^3) is the volume of water; Q (m^3/a) is the flow in and out of the system
 537 at equilibrium; Ce (g/m^3) is the contamination concentration in the inflow (g/m^3); C
 538 is the pollutant concentration; Sc denotes other external pollution sources (m^3/a); and
 539 $r(c)$ is the reaction rate of pollutants in water ($g/m^3/a$). The above equation can be
 540 defined as the basic mass balance of a water body in a completely mixed system.
 541 Because the pollutants are evenly mixed in each small interval, the horizontal and
 542 vertical concentration gradients of pollutants can be neglected. Therefore, the model of
 543 water quality in mixed rivers under steady-state design conditions is adopted (Yue et
 544 al., 2021):

$$545 \quad W_c = 31.54 * [C_s \cdot (Q_p + Q_E + Q_S) - Q_p \cdot C_p] \quad (34)$$

546 where W_c represents the water environmental capacity (t/a); Q_p is the flow in the
 547 reach (m^3/s); C_p is the pollutant concentration in the river (mg/L); Q_E is the sewage
 548 discharge (m^3/s); Q_S is the total flow of nonpoint sources into the reach above the

549 control section (m^3/s); and C_s is the target concentration of river pollutants (mg/L).

550 The result calculated based on the total hydrological capacity standard is often

551 relatively large, which is generally referred to as nonconservative. To conform to real

552 conditions, the concept of a nonuniform coefficient is introduced for correction:

$$553 \quad W'_c = \alpha \cdot W_c = 0.6 \cdot W_c \quad (35)$$

554 This coefficient is used to assign a punishment if the water quality exceeds the

555 relevant value in a given sub-region. Based on the coefficient value, the objective

556 functions and constraints are adjusted accordingly. Finally, the daily decision

557 alternatives for water allocation from water departments to water users are obtained at

558 the regional decision level.

559 2.3.1 Objective function of the third layer

560 **Regional objective function: maximization of the comprehensive benefits of each**

561 **sub-region**

$$562 \quad \max f_3(x) = \sum_{t=1}^T \sum_{i=1}^I \sum_{j=1}^{J_r} x_{ij}^t b_{ij} - \sum_{j=1}^{J_r} \left(D_j - \sum_{t=1}^T \sum_{i=1}^I x_{ij}^t \alpha_{ij} \right) \times \omega_j - P_r(r_{nz}) - G_r(x_{ij}^t) \times q \quad (36)$$

$$563 \quad P_r(r_{nz}) = e_i \times \sum_{p=1}^{\text{Pr}} P_p^{\text{pump}} \times \nabla t_r + x_{ij}^t \delta_{ij} \psi_{ij} \omega_{ij} \quad (37)$$

$$564 \quad \nabla t_r = \sum_{t=1}^T \sum_{n=1}^N \sum_{z=1}^{Z_r} \left\{ \left(l_{nz} + \left(r_{nz}^t \theta_{nz} / \text{CAS}_{nz} \right) \right) / \left(Q_{nz}^{\max} / \text{CAS}_{nz} \right) \right\} / 3600 \quad (38)$$

$$565 \quad G_r(x_{ij}) = \sum_{z=1}^{Z_r} \sum_{u=1}^U \left(Q_{z,u,r}^{\text{final}} - Q_{z,u,r}^0 \right) \quad (39)$$

566 where b_{ij} (Chinese Yuan/ m^3) is benefit per unit of water supply for the j th user; ω_j is

567 the penalty coefficient per unit of water deficiency; $j=1,2,\dots,Jr$; Jr is the number of
 568 water users in r th sub-region; $r=1,2,\dots,R$; $P_r(r_{nz})$ is the penalty function for cost in
 569 the r th sub-region; e_i (Chinese Yuan/kW·h) is the unit electricity fee; P_p^{pump} (kW·h)
 570 is the electrical power consumed by the p th pump at a pump house in each hour; p
 571 ranges from 1 to Pr ; Pr is the total number of pumps in the r th sub-region; ∇t_r (h) is
 572 the time required for water transfer to provide support for the inland river flow in the
 573 r th sub-region; ω_{ij} (Chinese Yuan) denotes to the fee paid for sewage treatment; l_{nz}
 574 (m) is the length of a water diversion pipe from reclaimed water source n to the z th
 575 inland river; z ranges from 1 to Zr ; Zr denotes the number of inland rivers in the r th
 576 sub-region; CAS_{nz} (m²) is the cross-sectional area of a pipe from the n th reclaimed
 577 water source to the z th inland river; Q_{nz}^{\max} (m³) is the maximum overflow capacity of
 578 the diversion pipe from the n th reclaimed water source to the z th inland river; $G_r(x_{ij})$
 579 is the penalty function for substandard water quality in the r th sub-region; $Q_{z,u,r}^{final}$ (mg/L)
 580 is the final concentration of the u th pollutant in the control section of the z th inland river
 581 in the r th subregion after optimal configuration; $Q_{z,u,r}^0$ (mg/L) is the initial
 582 concentration of the u th pollutant in the z th inland river in the r th sub-region; and q is
 583 the penalty coefficient for substandard water quality in the r th sub-region. The number
 584 of objective functions in this layer depends on the number of sub-regions divided in the
 585 city, which is based on local conditions.

586 **2.3.2 Constraints of the third layer**

587 **Water quality constraints**

588 Mathematical models are often developed to help satisfy the water quality standards at
589 monitoring points (Zhang et al., 2019; Pourshahabi et al., 2020; Friesen et al., 2017).

590 However, for some cities with very few monitoring points, such approaches may lead
591 to good water quality in the monitored sections and poor water quality in other sections.

592 In these circumstances, the quality of water bodies in each sub-region of a city is not
593 simultaneously maintained. To maintain the water quality in all sub-regions of a city at
594 the desired target level, the water quality constraint in Eq. (40) is established:

$$595 \quad Q_{z,u,r}^{final} \leq Q_{z,u,r}^{control} \quad (40)$$

596 where $Q_{z,u,r}^{control}$ (mg/L) denotes the control standard for the u th pollutant in the control
597 section of the z th inland river in the r th sub-region.

598 **2.4 Model solution**

599 **2.4.1 Synergy degree evaluation**

600 Enhancing the understanding of the synergy among water allocation alternatives to
601 achieve broad coordination and equilibrium is crucial. The evaluation of the synergy of
602 a complex water resources system is strongly related to multiple complex interactions,
603 such as the interactions among different processes, users, and regions. However, these
604 interactions have rarely been explicitly captured in prior evaluations of water allocation.

605 One of the key network metrics used in network analysis, connectivity, is a promising
606 measure of the degree of coordination among different objectives in complex systems
607 (Weitz et al., 2018). Connectivity reflects the connectedness of a given link to all
608 possible links in the network, and the strength of each link is weighted, reflecting the
609 number and strength of correlations (Felipe-Lucia et al., 2020). In this study,
610 connectivity is used to embody coordination in the context of synergy, as shown in Eq.
611 (26). Due to the limited supply of water resources, competition among different
612 objectives is unavoidable, and the objectives cannot be fully optimized to equal extents,
613 i.e., an increase in one target output may decrease another output. Therefore,
614 equilibrium is integrated as another vital part of the synergy devoted to maintaining a
615 balance among the satisfaction of each goal in a system. The equilibrium based on the
616 principle of information entropy (Gao et al., 2013; Zivieri, 2022) is shown in Eq. (27).
617 Information entropy is a measure of the uncertainty associated with a random variable
618 and is used to quantify the information contained in a message, usually in bits or
619 bits/symbols; furthermore, it has been widely used to represent the fairness or
620 equilibrium of a system (Chen et al., 2022; Zhao et al., 2022). When H is low, the level
621 of equilibrium in the system is high. This factor is also used to be compared with the
622 proposed index. By combining the quantification of coordination and equilibrium, the
623 synergy degree is appropriately determined (Eq. (29)). Notably, the total synergy index
624 (TSI) of a system is used for both generating candidate management alternatives in the
625 generation phases of PTSOA and performing assessments of the associated level of

626 synergy, as shown in Eqs. (41-44).

$$627 \quad SSI_{ob_i} = \frac{\sum_{j=1}^N c_{ij} \times (ob_i + ob_j)}{\sum_{j=1}^N (ob_i + ob_j)}, i \neq j \quad (41)$$

$$628 \quad (42)$$

$$629 \quad u_{ob_i} = \frac{ob_i - ob_{i,\min}}{ob_{i,\max} - ob_{i,\min}} \quad (43)$$

$$630 \quad TSI = \frac{\sum_{i=1}^N SSI_{ob_i}}{H(S)} \quad (44)$$

631 where SSI_{ob_i} is the connectivity of the i th object; c_{ij} is the Pearson correlation
632 between the i th object and j th object; ob_i and ob_j are the values of the i th and j th
633 objective functions, respectively; $H(S)$ is the overall equilibrium of all objects based
634 on the principle of information entropy, and it is abbreviated as H in the following;
635 u_{ob_i} is the standardized value of the i th object; N is the total number of objects in the
636 system; $ob_{i,\min}$ and $ob_{i,\max}$ are the minimum and maximum critical thresholds of the
637 parameter ob_i , respectively. SSI is ranged from 0~ N , and higher SSI indicates higher
638 connectivity of the objects in the system which means they are easier to promote each
639 other. H is ranged from 0~ $N \cdot \log(1/N)$ and lower H indicates better overall equilibrium
640 from objective perspective. TSI is greater than 0. When a water resource system's TSI
641 value is higher, the degree of synergy is higher. In our application, based on actual
642 evaluation, we define when $TSI \geq 5$, the degree of synergy is considered satisfactory.
643 $5 > TSI \geq 3$ is defined as moderate and $3 > TSI$ is defined as low.

644 **2.4.2 Hierarchical optimal algorithm design for the PTSOA model**

645 Based on the algorithm design with a hierarchical objective function proposed by Li et
646 al. (2022), a new level is added to the original two levels of the algorithm, and the
647 alternative generation phase is improved for better synergy. In this algorithm, the
648 objective functions in the upper decision level is first satisfied, and then the lower-level
649 objective function provides an optimal result based on the results of optimal allocation
650 in the upper level. To provide as comprehensive solutions as possible, the decision
651 alternatives need to be classified into different sets for further selection. In addition, the
652 synergy degree of the result of each layer is calculated to select optimal decisions
653 among all Pareto front solutions. The detailed steps of the hierarchical optimal
654 algorithm are as follows:

- 655 I. In the first level, calculate the objective function (city level) values for the social,
656 economic and sustainable development components, and sort the results with
657 NSGA-III (Pourshahabi et al., 2020; Chen et al., 2017) to obtain each Pareto
658 front F_1, F_2, \dots, F_i .
- 659 II. Classify the Pareto fronts into K (K is determined based on the diversity of
660 policies) elements with the K-means algorithm (Liu et al., 2022), which is used
661 to partition a data set into K distinct and non-overlapping clusters. To perform
662 K-means clustering, we first specify the desired number of clusters K . Then, the
663 K-means algorithm is used to assign each observation to exactly one of the K
664 clusters.
- 665 III. Calculate the synergy degree of each individual in the front, and select the

666 solution that yields the greatest synergy in each cluster. K solutions are obtained
667 in the first layer.

668 IV. Use the selected K solutions in the first layer to establish constraints in the
669 second layer. Solve the objective function of the second layer with NSGA-III.

670 V. Calculate the synergy degree of each individual in the front and select the
671 solution that yields the greatest synergy as well as the two solutions that
672 maximize the conventional and unconventional water supply department
673 objective functions in all Pareto fronts with K preconditions.

674 VI. The three selected solutions in the second layer are used to establish constraints
675 in the third layer. Solve the objective function of the third layer with NSGA-III
676 under the three preconditions.

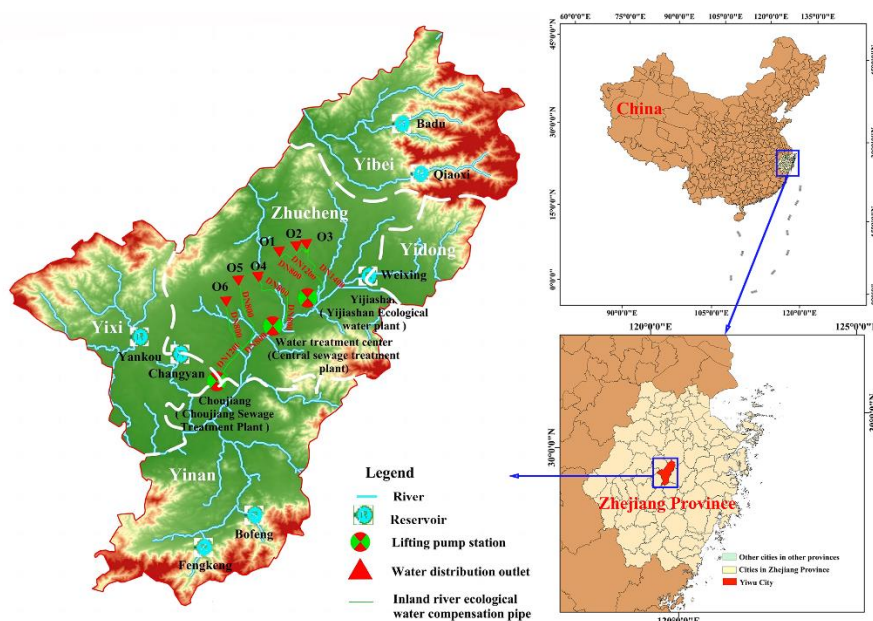
677 VII. The synergy degree of each individual in the front is calculated, and the solution
678 that yields the greatest synergy in the third layer is selected. Three solutions are
679 obtained considering the synergy in the former two layers. Finally, the
680 synergistic configurations optimal for all stages in the whole process are
681 identified considering the synergy among decision levels, processes and time
682 scales.

683 **3. Application**

684 **3.1 Study area**

685 Yiwu city is selected as a case study to validate the applicability of the PTSOA model.
686 This city is in Southeast China, located from 119°49 'E-120 °17' E and 29°02 '13 "N-
687 29 °33' 40" N and covers an area of 1105 km². The area is characterized by a scarcity
688 of water resources, and the conventional water supply is under severe stress. The
689 regional water consumption depends heavily on transported water and external water
690 transfer. The per capita water resource is in total 622 m³, which is only 22.6% of the
691 provincial average and 19.1% of the national average. Moreover, the problem of water
692 pollution has become a bottleneck constraint for the development of Yiwu city.
693 Therefore, it represents a typical water-scarce city with limited conventional water.
694 Notably, water quality in Yiwu has been subjected to significant environmental stress
695 because of the negative effects of wastewater discharge with the rapid development of
696 industry. The current water quality is poor, with Class *V*, and the main pollutant
697 concentrations exceed the corresponding standards (Zhejiang Natural Resources and
698 Statistical Yearbook on Environment, 2020). As shown in Fig. 3, the Yiwu River crosses
699 the city from northeast to southeast. Additionally, there are six ecological water
700 compensation outlets in six main tributaries in the Yiwu River. In Fig. 3, the white labels
701 indicate five sub-regions in the city, the black labels near the reservoirs are their names,
702 the black labels named O1~O6 indicate the name of the water distribution outlets and

703 the labels near the lifting pump station are their names.



704

705 **Fig. 3. Map of the study area**

706 **3.2 Generalization of the complex water resources system**

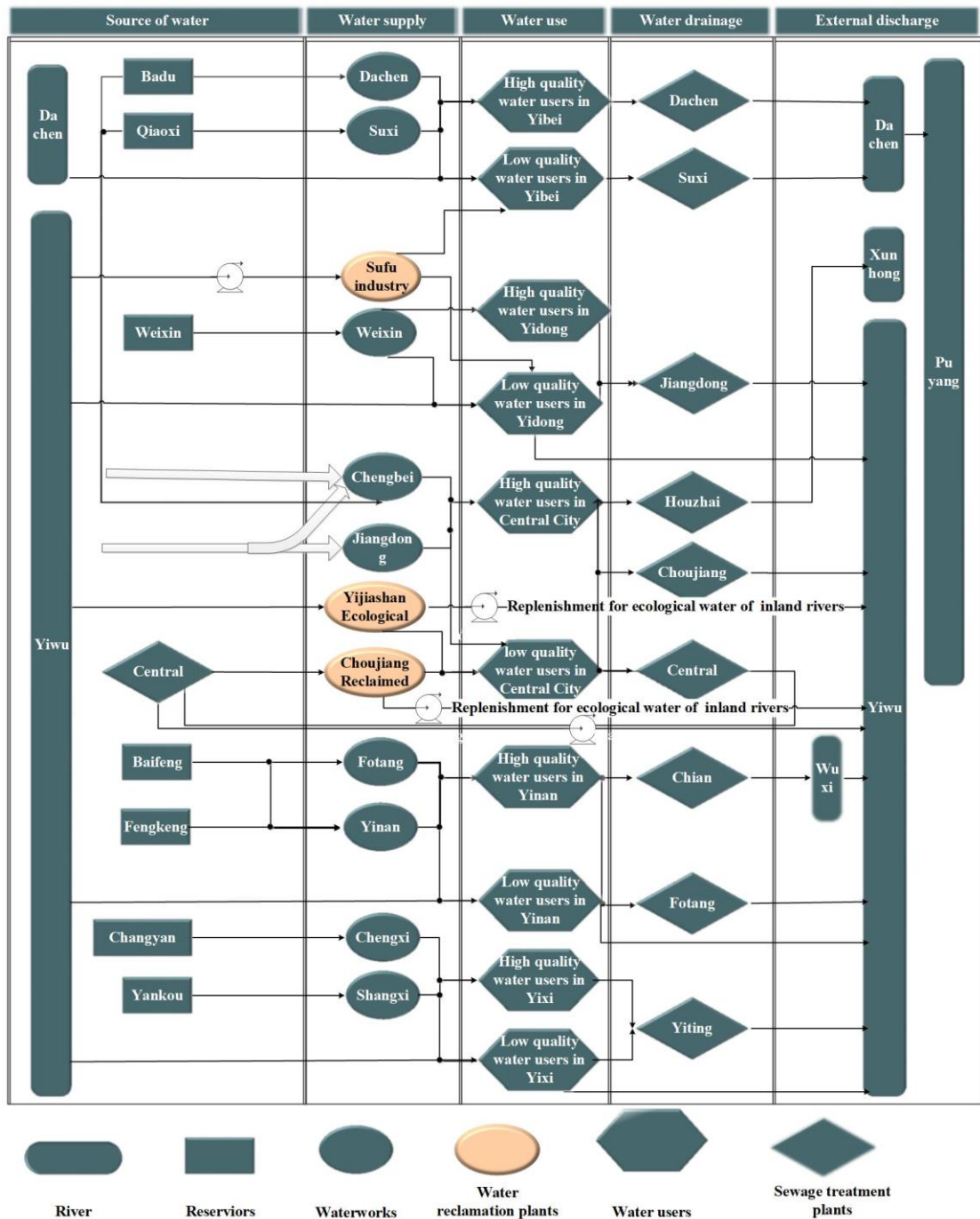
707 An initial multi-source, complementary and mutually regulated system has been
708 developed for Yiwu, and this system spans the entire urban water cycle (water source-
709 water supply-water use-drainage-drainage collection-recycling and reuse). To apply the
710 optimal water allocation model to the complex real-world water system, all
711 stakeholders in the complex water resources system should be schematized into a
712 topological system, as shown in Fig. 4. The diagram comprises five modules: water
713 sources, water supply, water use, water drainage and external discharge for all
714 stakeholders.

715 The first module includes seven main reservoirs, two water diversion projects, the

716 Central Sewage Treatment Plant and the Yiwu River. The seven reservoirs and two
717 water diversion projects (as shown in Table 1) supply high-quality water. There are
718 complex connections between the first and second modules. For example, two
719 reservoirs supply water to one waterworks or one reservoir feeds two or three
720 waterworks simultaneously. The reservoirs also supply some of the agricultural and
721 ecological waters to subareas of the city. The Yiwu River, with a total length of 38.39
722 km and 21 first-class tributaries in the city, and the Central Sewage Treatment Plant, as
723 shown in Table 2, are low-quality water sources. There are no data available for
724 agricultural irrigation water, and most agricultural irrigation water is supplied from
725 surface water stored in hundreds of small reservoirs and mountain ponds (Yiwu
726 Ecological Environment Status Bulletin, 2020). So, this water volume is ignored in the
727 model.

728 For the second module, high-quality water piped from reservoirs is transported to
729 nine urban and rural centralized waterworks (as shown in Table 2). The Yiwu River
730 distributes low-quality water to the Yijishan Ecological Water Plant and Sufu Industrial
731 Water Plant through the Yijishan and Baisha Water Pump Stations, respectively. The
732 water discharged at the Central Sewage Treatment Plant is transferred to the Choujiang
733 Industrial Water Plant. Based on the water supply project distribution and the economic
734 as well as social development levels, Yiwu is divided into five districts, as shown in
735 Table 3: the Central District, Yidong District, Yibei District, Yinan District and Yixi
736 District. The third module comprises both high-quality water users (high-quality water

737 users consist of urban and rural domestic water users and some industrial water users
738 in the water supply network of urban and rural public water plants) and low-quality
739 water users (low-quality water users include other industrial water users, municipal
740 water users and ecological water replenishment for inland rivers) in each district. There
741 are nine sewage treatment plants in the fourth module (which focuses on the drainage
742 stage), as shown in Table 2. The unreused water from sewage treatment plants is
743 discharged to the external environment. Reuse processes are also considered in the
744 system.
745



746

747

Fig. 4. Schematic diagram of Yiwu city

748 3.3 Parameter determination

749 According to the flow duration curve of the annual natural inflow data for 51 years

750 (1963-2014), three years with exceedance probabilities of 50%, 75% and 90% are

751 selected to represent normal (1984.1–1985.1, annual mean inflow: $1.33 \times 10^8 \text{ m}^3$), dry
 752 (2008.1–2009.1, annual mean inflow: $1.11 \times 10^8 \text{ m}^3$), and extremely dry (1971.1–
 753 1972.1, annual mean inflow: $0.63 \times 10^8 \text{ m}^3$) scenarios, respectively. In addition to
 754 inflow, the data used in the PTSOA model mainly include the data for the parameters
 755 in each layer. Water demand values were calculated using the Yiwu City Water
 756 Resources Comprehensive Plan 2020, as shown in Table 1.

757 **Table 1** Water demands of various regions in Yiwu in 2020 (10^4 m^3)

Subregion	Yibei	Yidong	Zhucheng	Yixi	Yinan
water demand	1695	572	11813	2198	2045

758

759 The water resources fees paid to the government are in total 0.3 Chinese Yuan/ m^3 .

760 The parameters of the reservoirs and external water division projects in Yiwu city are

761 listed in Table 2.

762 **Table 2** Parameters of the reservoirs and external water division projects

Reservoirs & External sources	Water Fee (Chinese Yuan/ m^3)	Initial storage (10^4 m^3)	Dead storage (10^4 m^3)	Flood limit	
				storage capacity (10^4 m^3)	Absolute storage capacity (10^4 m^3)
Badu	0.99	1359	49	2688	2639
Qiaoxi	1.30	1505	77	2933	2856
Weixin	0.37	500	17	483	466
Baifeng	1.05	1013	15	2010	1995
Fengkeng	1.15	778	55	1501	1446
Yankou	1.49	1820	499	3140	2641
Changyan	0.70	491	41	940	899
Pujiang Project	1.00	0	0	3000	3000
Dongyang Project	1.00	0	0	5000	5000

763 The Tennant method is applied to calculate the ecological water demand. In this

764 method, the relationship between the annual average discharge and habitat quality is
765 considered, and the percentage of the annual average natural runoff is used as the
766 recommended value of the ecological water demand for a given river channel.
767 According to the recommended values, the percentage of runoff required for the fish
768 spawning period from April to September is 30% and the percentage runoff in the
769 general water consumption period (October to March) is 10%.

770 Based on observations obtained with the F601 evaporator (a standard evaporation
771 instrument widely used in China), evaporation is calculated as:

$$772 \quad EP = E \times k \quad (45)$$

773 where EP (mm) is the evaporation of a reservoir; E (mm) is the observed evaporation;
774 and k is a reduction coefficient. According to observations, the difference of
775 this coefficient is quite slight within a small watershed (Zhao, 2014). Thus, k is
776 simplified to the same value 0.88 for every reservoir and varies throughout the year
777 according to expert experience (Zhao, 2014). The prices of conventional water and
778 reclaimed water are 1.7 and 2.6 Chinese Yuan/m³, respectively. In our application of the
779 model, this precipitation component associated with the water sources were calculated
780 by the Thiessen polygon method (Liu et al., 2014) based on the measured data of seven
781 rainfall stations (Shi Caotou, Suxi, Yiwu, Fotang, Baifeng, Fengkeng, Changfu) in the
782 basin in normal (1984.1–1985.1), dry (2008.1–2009.1), and extremely dry (1971.1–
783 1972.1) scenarios.

784 The monthly mean monitoring data for effluent pollutant concentrations and the

785 daily maximum processing capacities of sewage treatment plants were obtained from
786 the monitoring systems of the sewage treatment plants. For example, the concentrations
787 of COD, NH₃-N, TN, and TP in the sewage of the Jiangdong Sewage Treatment Plant
788 are 13.80 (mg/L), 0.22 (mg/L), 6.02 (mg/L), and 0.13 (mg/L), respectively. The daily
789 maximum processing capacity of Jiangdong Sewage Treatment Work is 12 (10⁴ t/d).
790 The effluent quality of sewage treatment works satisfies Class A Standard used in China.
791 The maximum capacities of the Baisha pump station, Yijiashan pump station,
792 Choujiang pump station and water treatment centre pump station are 13 t/d, 13.5 t/d, 10
793 t/d, and 4.5 t/d, respectively.

794 Additionally, the environmental capacities of the six tributaries that are replenished
795 with ecological water are calculated according to Eqs. (33)-(35), and the results are
796 listed in Table 3. COD, TP and TN are major pollutants in Yiwu City (Yiwu Ecological
797 Environment Status Bulletin, 2020), and they are also major controlled pollutants of all
798 the monitoring sections. So, they were selected as representative pollutants in the
799 tributaries to guarantee the water environmental quality of inland rivers. The water
800 quality goals for the tributaries must conform to Class III standard according to GB
801 5749-2006 in China. The unit electricity price of pump stations in Zhejiang Province is
802 0.41 Chinese Yuan/kW · h. GB50014-2006 (2014 edition) stipulates that the
803 comprehensive urban domestic sewage quota should be 80~90%, and the urban
804 comprehensive domestic sewage quota should be 90% in areas with extensive drainage
805 facilities. There are many influencing factors in the model and the most important ones

806 among them are the value of water demand, the value of available water and some key
807 hyper-parameter. According to the “Jinhua Water Resources Bulletin (2020)”, the urban
808 comprehensive domestic sewage quota is set to 90%, and the sewage treatment rate is
809 set to 100%. The benefits per unit water supply for different users in different
810 subregions are determined from the Yiwu Water Price Adjustment Plan (2020).

811

812 **Table 3** Area and environmental capacity of tributaries

Name of tributary	Area (km ²)	Class III		
		COD (t/a)	TN (t/a)	TP (t/a)
Chengdong	3.4	188.1	4.7	0.4
Chengzhong	8.7	432.7	31.5	3.8
Chengxi	6.3	302.5	9.5	2.3
Chenganan	7.1	318.8	0	3.6
Hongxi	12.5	778.8	138.8	7.9
Dongqingxi	38	1271.4	221.5	12.7

813 **4. Results and discussion**

814 By solving the PTSOA model for Yiwu city, synergistic optimal water allocation results
815 for different layers (across different decision levels, water use sectors, and sub-regions)
816 are obtained under normal, dry and extremely dry conditions. Pareto sets are obtained
817 across 500 runs and 1000 iterations (in most cases) of the PTSOA model with the
818 proposed hierarchical optimization algorithm. If the feasible solutions could not be
819 found in some cases, the number of iteration would be increased. It took approximately
820 34 h of CPU time on a computer with 32 GB memory and intel corei7@3.4 GHz of
821 CPU. Therefore, in this study, each iteration for a single trial solution takes 0.24 s of

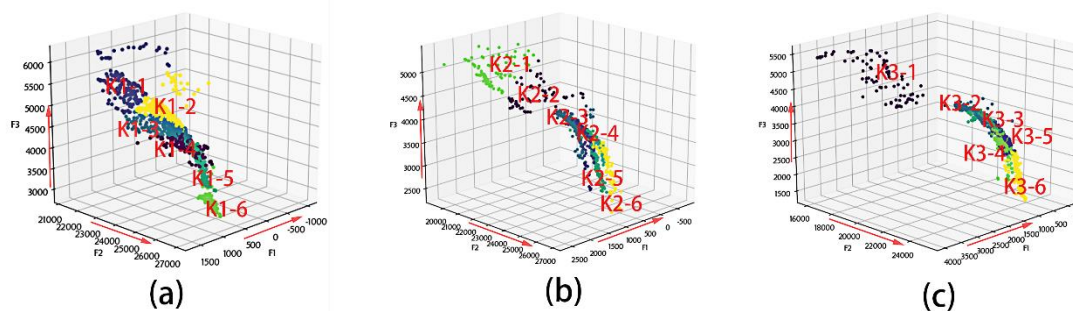
822 CPU time on the computer with the named specifications.

823 **4.1 First layer of the PTSOA model for synergistic optimal** 824 **water allocation**

825 To demonstrate the relationship among conflicting objectives, sets of Pareto solutions
826 for the first layer under normal, dry and extremely dry conditions are shown in Fig. 5.
827 In each of the figures, the total water supply shortage, total water supply benefit and
828 total amount of water retained in reservoirs in Yiwu city are plotted. The colour of the
829 markers indicates the classification of the solutions of the K-means method, as
830 described in Section 2.4.2. All of the decision alternatives are classified into six groups
831 marked in different colours for broad-scale decision-making. The names of the classes
832 are marked in the figure in red (for example, K1-1 represents the first class of solutions
833 in the normal scenario, and K3-2 represents the second class of solutions in the
834 extremely dry scenario). The red arrows indicate optimization directions. The ideal
835 solution is located at the top-right corner (low total water supply shortage, high total
836 water supply benefit, and relatively high total amount of reserved water in reservoirs)
837 of the plot. The geometries of the trade-offs vary significantly across the applications,
838 as is expected given different hydrological conditions. Generally, the total water supply
839 shortage and the total amount of water retained in reservoirs show an inverse
840 relationship. In contrast, the total water supply benefit shows a direct and positive
841 influence on the total water supply shortage. The water shortage varies in the range of

842 $-1.2 \times 10^6 \sim 0.8 \times 10^5 \text{ m}^3$, $-0.5 \times 10^5 \sim 2.0 \times 10^6 \text{ m}^3$, $0 \sim 3.5 \times 10^6 \text{ m}^3$ in normal, dry and
843 extremely dry scenarios respectively. The average water demand is around $1.8 \times 10^8 \text{ m}^3$,
844 and water shortage of the selected decision alternatives are all less $9 \times 10^6 \text{ m}^3$. So, the
845 water supply reliability of the selected decision alternatives is greater than 95% under
846 normal, dry and extremely dry conditions with the consideration of water demand. The
847 total amount of reserved water in reservoirs under normal scenarios varies in the range
848 of $2.91 \times 10^7 \text{ m}^3$ to $6.14 \times 10^7 \text{ m}^3$, which is much higher than that under the extremely dry
849 scenario, with a value of $1.44 \times 10^7 \text{ m}^3$ to $2.93 \times 10^7 \text{ m}^3$. This finding demonstrates that
850 the optimal allocation is able to reconcile the present demand and future needs, even in
851 extremely dry scenarios. The total water supply shortage in all scenarios is less than 5%
852 of the water demand, which indicates that the guaranteed water supply is greater than
853 95%.

854



855

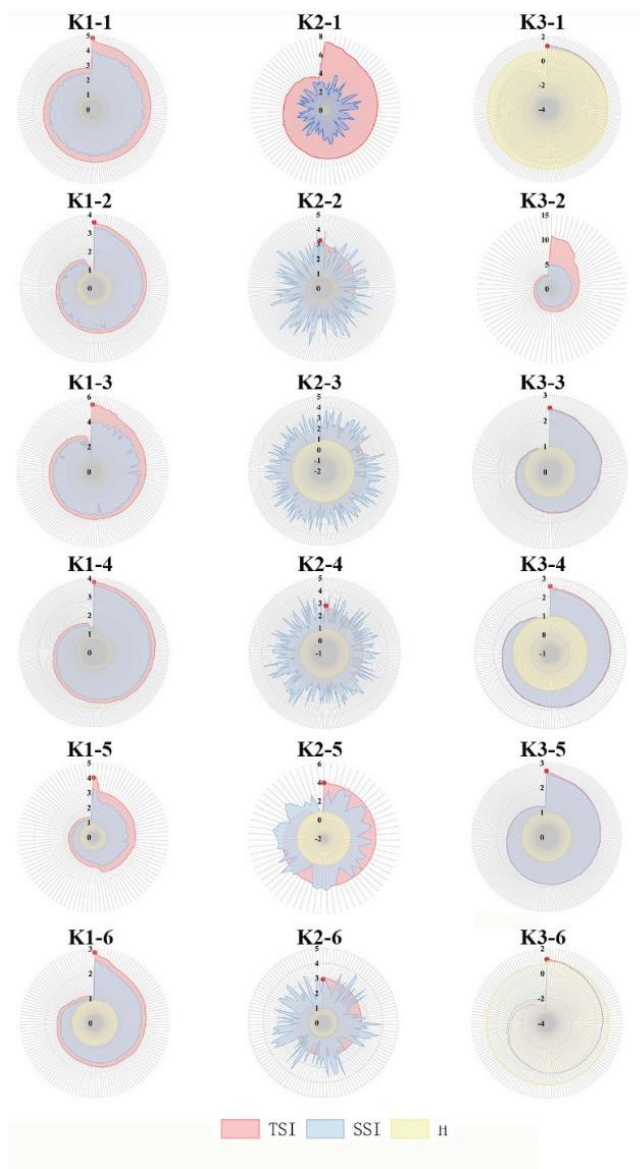
856 Fig. 5. Sets of Pareto solutions after 500 model simulations with the hierarchical
857 optimal algorithm under (a) normal, (b) dry and (c) extremely dry scenarios. (F1: total
858 water supply shortage, 10^4 m^3 ; F2: total water supply benefit, 10^4 Chinese Yuan; F3:
859 the total amount of reserved water in reservoirs, 10^4 m^3 . The red arrow indicates the

860 direction of optimization. K1-n, K2-n and K3-n represents the nth class of solutions
861 in the normal, dry and extremely dry scenario separately, n=1~6.)

862 We further present the *TSI*, *SSI* (total connectivity) and *H* (overall equilibrium)
863 values for different classes characterized based on the optimal PTSOA solutions under
864 three scenarios, as shown in Fig. 6. In the PTSOA model, the Pareto solutions with the
865 best *TSI* values are input to the second layer for further optimization. Thus, the red
866 points in Fig. 6 represent the selected schemes for all classes. We observe that the
867 variation in the *TSI* is consistent with that in the *SSI* in some, but not all cases. In some
868 cases, differences are mainly caused by the influence of *H*, which influences the optimal
869 hydrological equilibrium, especially in dry condition. These results suggest that when
870 water is very limited, equally limited water is supplied to all users, thus enhancing the
871 overall equilibrium. We note that the *SSI* value is higher in the normal scenario than in
872 the other two scenarios. We attribute this to relatively abundant water being useful for
873 stakeholders to achieve synergy due to the reduced competition compared to other cases.
874 The *TSI* values reach maximums of 5.36, 7.37 and 10.82 under normal, dry and
875 extremely dry conditions, respectively.

876 In Fig.6, the value of *TSI* are significantly diverse among different scenarios as
877 well as different solutions. *H* is widely used to evaluate the equality of different
878 solutions (Gao et al., 2013;Li et al., 2022). As a contrast, the value of *H*, which is used
879 for comparison and construction of *TSI*, show slight differences among solutions and
880 even are the same in some classes. Therefore, it is difficult for decision makers to select

881 the best solution among all candidates if we only use H for evaluation and selection in
 882 the decision process. Compared to H , TSI introduces SSI into evaluation and the
 883 difference of coordination relationship between different schemes is distinguished by
 884 SSI . But H only pays attention to the equity among the stakeholders. So, TSI is more
 885 effective and valid than H in some extent. Additionally, since TSI is used to illustrate
 886 the synergy of allocation plans under certain conditions, the three kinds of TSI values
 887 are not comparable.

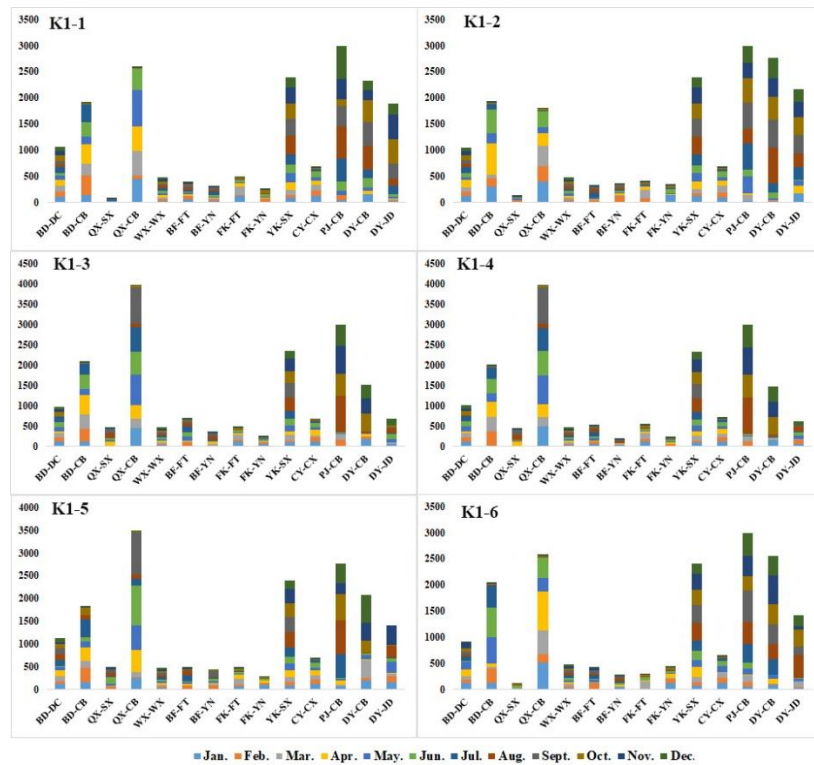


888

889 Fig. 6. Comparison of *TSI* (total synergy index), *SSI* (total connectivity) and *H*
890 (overall equilibrium) values among various Pareto solutions in different classes for
891 the (K1) normal, (K2) dry, and (K3) extremely dry scenarios. (K1-n, K2-n and K3-n
892 represents the nth class of solutions in the normal, dry and extremely dry scenario
893 separately, n=1~6.)

894 As an example, Fig. 7 provides the specific water supply decision alternatives for
895 the first layer that maximize synergy in each cluster under normal conditions. The water
896 allocation plans for the seven main reservoirs and two external water diversion projects
897 in every month of the configuration period are displayed. All reservoirs and water works
898 are represented by abbreviations based on their full names in Fig. 7. For example, QX-
899 CB is the label for the water supplied from Qiaoxi Reservoir to Chengbei Water Works.
900 The water volumes supplied by Qiaoxi Reservoir to Chengbei Water Works (ranging
901 from 1.78×10^7 m³ to 3950×10^4 m³) and from the Pujiang External Water Division
902 Project to Chengbei Water Works (ranging from 2.57×10^7 m³ to 3×10^7 m³) are relatively
903 high in all clusters. This result is consistent with the fact that Chengbei Water Works is
904 one of the main conventional water sources for the central city area, a region that
905 accounts for more than 50% of the total water demand of Yiwu city. The water supplied
906 by the two external water diversion projects from August to December is higher than
907 that in other months. The mean monthly precipitation in these months is only 58-74%
908 of the mean annual precipitation in Yiwu, so more external water is supplied for
909 replenishment. Baifeng and Fengkeng Reservoirs supply similar volumes of water to

910 their two connected waterworks.



911

912 **Fig. 7.** Water supply from each reservoir to connected water works in each month in

913 the normal scenario 10^4 m^3

914 (K1-n represents the n^{th} class of solutions in the normal scenario, $n=1\sim 6$.)

915

916 **4.2 Second layer of the PTSOA model for synergistic optimal** 917 **water allocation**

918 The 6×3 decision alternatives selected in the six clusters of the optimal first-layer results

919 in the scenarios are inputs into the second layer for further optimization. As shown in

920 Fig. 8, the total amount of water retained in water works and the amount of

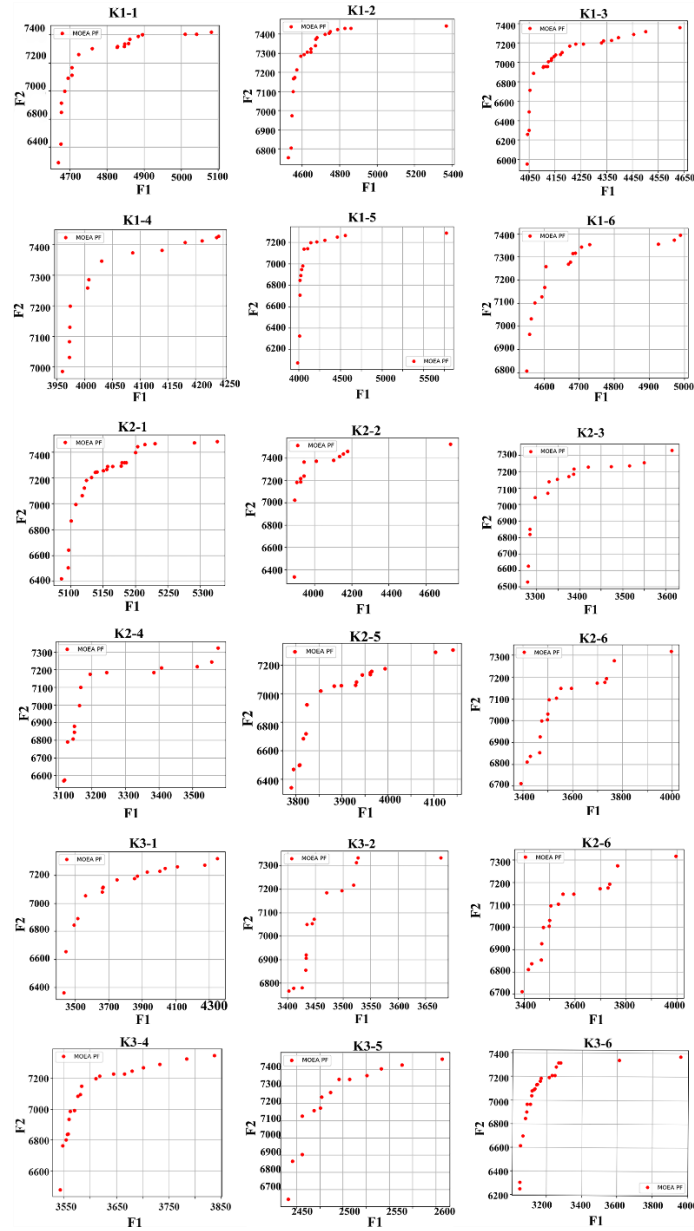
921 unconventional water supplied show a negative correlation. In the alternative

922 generation phase of game bargaining between the two objectives, the greater the total
923 amount of water retained in water works is, the greater amount of unconventional water
924 will be supplied, which indicates that more conventional water will be saved when more
925 unconventional water is supplied. Conversely, the amount of unconventional water
926 supplied is affected by the total amount of water retained in water works.

927 In the second layer, three alternatives in each scenario are selected as prior
928 conditions for further optimization. In addition to the two individual extrema of the two
929 objectives, the alternative that yields the best synergy is also identified, and it is similar
930 to that in the first layer. In the normal scenario, the *TSI* values are -0.90, -1.02 and -0.88
931 in the cases with the optimal conventional water supply, unconventional water supply
932 and synergy, respectively. The most synergistic approach includes 7.08×10^4 m³ more
933 conventional water retained than that in the conventional water supply cases and
934 9.72×10^4 m³ more than that in the optimal unconventional water supply case. Therefore,
935 not only is the best *TSI* value obtained, but the requirements of both conventional and
936 unconventional water supply departments are met.

937 Overall, the total amount of water retained in the water works ranges from 3.95×10^7
938 m³ to 5.75×10^7 m³, 3.12×10^7 m³ to 5.31×10^7 m³, and 2.43×10^7 m³ to 3.96×10^7 m³ for the
939 three types of conditions. The total amount of unconventional water supplied ranges
940 from 5.95×10^7 m³ to 7.48×10^7 m³, 6.34×10^7 m³ to 7.56×10^7 m³, and 6.28×10^7 m³ to
941 7.37×10^7 m³ in the normal, dry and extremely dry scenarios, respectively. Moreover, by
942 selecting the solution with the highest *TSI*, 7.35×10^7 m³, 7.56×10^7 m³, and 7.37×10^7 m³

943 of unconventional water would be supplied as an effective supplement to conventional
944 water. In the other word, conventional water would be saved by our proposed model
945 and index in the three scenarios. It is notable that the drier the conditions are, the lower
946 the amount of water retained in water works and the greater the amount of
947 unconventional water supplied. Thus, this approach is useful for cities to mitigate the
948 risk of drought. Additionally, based on the constraints regarding the contaminants
949 allowed to be discharged, more than 1272.21 t and 48.81 t of COD and ammonia
950 nitrogen emissions are avoided per year.



951

952 **Fig. 8.** Pareto fronts of the second layer in the PTSOA model after 500 simulations

953 with the hierarchical optimal algorithm in the normal, dry and extremely dry

954 scenarios. (F1 represents the total amount of water retained in water works , 10^4m^3 ; F2

955 represents the amount of unconventional water supplied, 10^4 m^3 . The direction of

956 optimization is from the top-right corner to the bottom-left corner. K1-n, K2-n and

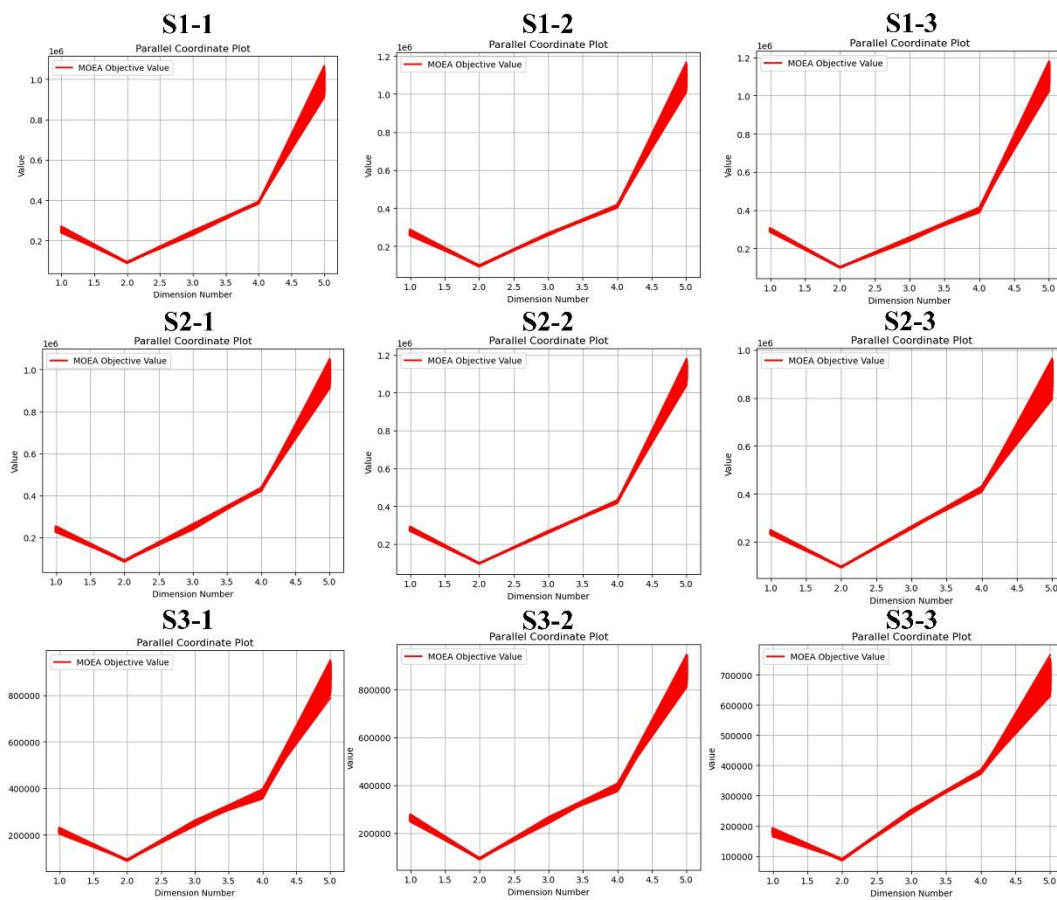
957 K3-n represent the n^{th} class of solutions in the three scenario respectively, $n=1\sim 6$.)

958 **4.3 Third layer of the PTSOA model for synergistic optimal** 959 **water allocation**

960 Fig. 9 shows the trade-offs among the five objectives in the third layer of the PTSOA
961 model for the (S1) normal, (S2) dry, and (S3) extremely dry scenarios (these
962 abbreviations are used to distinguish these results from those of the above two layers).
963 The number following ‘-‘ represents the selected solution from the second layer. For
964 example, S1-1 represents the normal scenario with the minimum total amount of water
965 retained in water works, S1-2 represents the normal scenario with the maximum
966 unconventional water supply and S1-3 represents the normal scenario with the
967 maximum synergy degree in the second layer. In each of these plots, the abscissa
968 denotes the identifier for the objective functions, which ranges from 1 to 5, and the
969 ordinate gives the objective values in the Pareto fronts (10^4 Chinese Yuan). The five
970 dimensions include the comprehensive benefits of the Yibei (1.0 dimension), Yidong
971 (2.0 dimension), Yixi (3.0 dimension), Yinan (4.0 dimension) and central city (5.0
972 dimension) sub-regions. As shown in the figure, the central city achieves the most
973 comprehensive benefit among the five sub-regions. This is primarily attributed to the
974 large population and intensive industry in this area. However, the benefits in the other
975 four sub-regions are also high compared to recent levels and those achieved with
976 traditional allocation methods, as shown in Table 9. Interestingly, the comprehensive
977 benefits in the sub-regions are greater in the scenario with the maximum synergy degree

978 under normal conditions than in the other two scenarios. The total comprehensive
 979 benefits in the five sub-regions in this scenario are approximately $2.3 \times 10^8 \sim 5.1 \times 10^8$
 980 Chinese Yuan higher than those in other cases, which indicates that the solution with
 981 the highest synergy degree in the second layer is the best choice for managers in normal
 982 years.

983



984

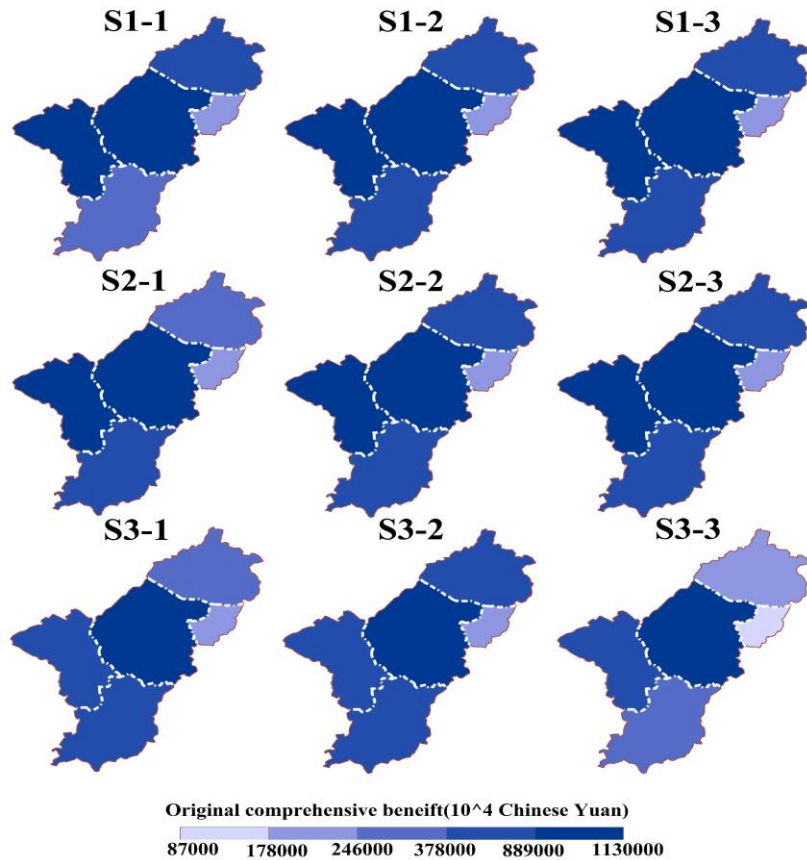
985 **Fig. 9.** Illustration of parallel-reference Pareto sets from the third layer in the
 986 PTSPOA model attained across all runs for the (S1) normal, (S2) dry, and (S3)
 987 extremely dry scenarios (S1-1 represents the normal scenario with the minimum total
 988 amount of water retained in water works, S1-2 represents the normal scenario with the

989 maximum unconventional water supply and S1-3 represents the normal scenario with
990 the maximum synergy degree in the second layer)

991

992 Fig. 10 presents the optimal comprehensive benefit in each sub-region. In all
993 scenarios, the central city is associated with the highest comprehensive benefit,
994 followed by Yixi and Yinan, and the comprehensive benefit in Yidong is relatively low.
995 This result may be related to Yidong which has the smallest area (72.2 km^2) and the
996 smallest population (7.7×10^4). Among the three normal decision alternatives, F1, F2
997 and F5 are highest in S1-3, with values of 3.03×10^9 Chinese Yuan, 9.90×10^8 Chinese
998 Yuan and 1.12×10^{10} Chinese Yuan, respectively. This indicates that considering the
999 synergy degree could increase the comprehensive benefit in most sub-regions in the
1000 normal scenario. Among the alternatives in the dry and extremely dry scenarios
1001 (excluding F4 and F5), other objectives are highest in S2-2, with values of 2.84×10^9
1002 Chinese Yuan, 9.63×10^8 Chinese Yuan and 2.67×10^8 Chinese Yuan, respectively. It
1003 suggests that maximizing the unconventional water supply is beneficial for the system
1004 in dry conditions. Additionally, F4 is highest, with a value of 2.29×10^9 Chinese Yuan,
1005 in S2-3 among the three solutions in the dry scenario, and F5 is highest, with a value of
1006 9.17×10^9 Chinese Yuan, in S3-1 in the extremely dry scenario.

1007



1008

1009

1010

1011

1012

1013

1014

1015

1016

Fig.10. Comprehensive benefit in five sub-regions after the regional collaborative allocation of water resources (S1 represents normal scenario, S2 represents dry scenario, and S3 represents extremely dry scenarios; S1-1 represents the normal scenario with the minimum total amount of water retained in water works, S1-2 represents the normal scenario with the maximum unconventional water supply and S1-3 represents the normal scenario with the maximum synergy degree in the second layer)

1017

4.4 Discussion

1018

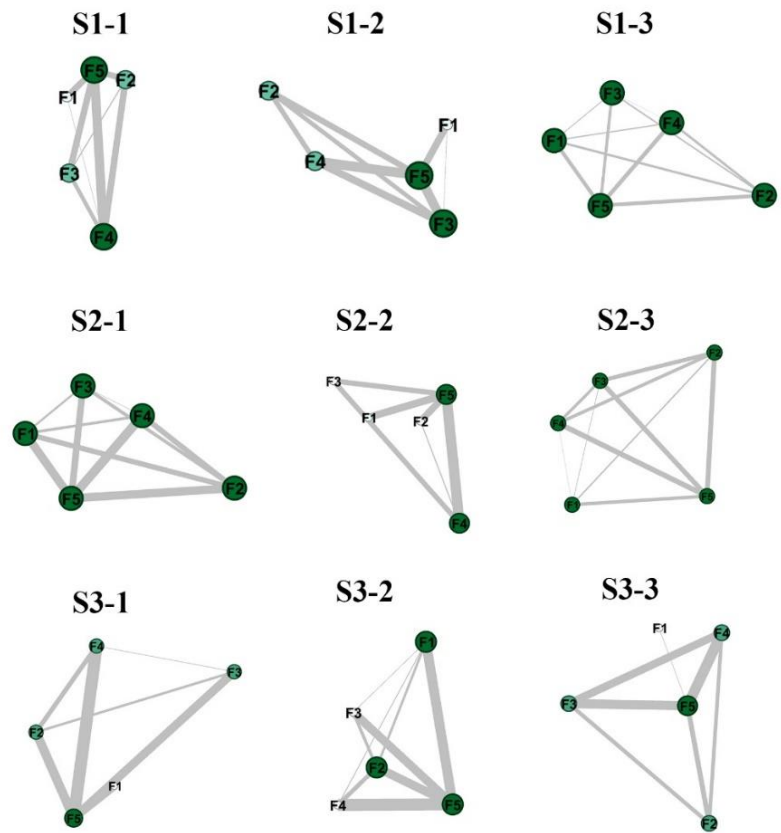
To assist policymakers in understanding the complex and systemic nature of complex

1019

water resources systems and reveal the dynamic interactions among objectives, network

1020 analysis and optimization were applied. Complex network analysis helps reveal the
1021 interactions among three layers with different dimensions. We determine the level of
1022 synergy in complicated water systems, identify the challenges and opportunities for
1023 sustainable development of water systems in cities with various subregions, and provide
1024 valuable insights and specific action priorities for these regions.. In the networks shown
1025 in Fig. 11, each node represents an individual objective (F1, F2, F3, F4, and F5 represent
1026 the comprehensive benefits in Yibei, Yidong, Yixi, Yinan and the central city,
1027 respectively), and pairwise objectives that are significantly ($P < 0.05$) correlated are
1028 connected by a link, where the strength of each link is related to the Pearson correlation
1029 coefficient. The obtained networks with five nodes were weighted and undirected
1030 (directionality can be estimated only if the direction of causality is known). The size of
1031 the circles in the figure indicates the connectivity of each objective. We considered
1032 trade-offs (i.e., negative correlations wherein one objective improves while the other
1033 worsens) among the objectives. In most scenarios, F5 was the relatively dominant
1034 objective, signifying that other objectives disproportionately deteriorated as progress
1035 was made towards the benefit of the central city, as shown in Fig. 11. It is evident that
1036 the trade-offs are more balanced in the scenarios with the highest degrees of synergy
1037 (S1-3, S2-3, and S3-3), which indicates that the trade-offs and competitions among the
1038 objectives are alleviated when synergy is considered. The links show that the conflicts
1039 of interest between F4 and F5 in scenarios S1-1 and S2-2 are extremely notable,
1040 suggesting that the comprehensive benefits in Yinan and the central city correspond to

1041 strong negative interactions in these cases. The connectivity of most objectives was
 1042 relatively low in the trade-off network in the extremely dry scenario, but F5 played a
 1043 dominant role in terms of negative interactions among objectives.. Moreover, as the
 1044 scenario varied from normal to extremely dry, the impact of individual regional targets
 1045 on the whole system diminished.



1046

1047

Fig. 11. Network analysis of the results of Layer 3

1048

(The circles of F1,F2, F3, F4 and F5 represent the connectivity of each comprehensive

1049

benefit of Yibei, Yidong, Yixi, Yinan and the central city, respectively:S1 represents

1050

normal scenario, S2 represents dry scenario, and S3 represents extremely dry

1051

scenarios, S_{m-1} represents the normal scenario with the minimum total amount of

1052 water retained in water works, S_{m-2} represents the normal scenario with the
1053 maximum unconventional water supply and S_{m-3} represents the normal scenario with
1054 the maximum synergy degree in the second layer, $m=1\sim3$)

1055

1056 For comparison, we applied six widely used MOEAs, namely, NSGA-II, SPEA-II,
1057 ϵ -MOEA, IBEA, MOEA/D and Borg MOEA to solve cases with 3+2+5 mathematical
1058 objectives (3 objectives in the first layer, 2 objectives in the second layer and 5
1059 objectives in the third layer) with the same constraints given previously for Yiwu city
1060 under normal, dry and extremely dry conditions. The constraints and common
1061 parameters, such as the maximum number of model simulations and the simulated
1062 binary crossover (SBX) rate, are set to those used in the PTSOA model. However, it is
1063 difficult to determine feasible decision alternatives with MOEAs, even though the
1064 number of iterations is increased to 20000 (which is far beyond that considered in the
1065 previous modelling) because the complexity of the system overshadows the
1066 optimization capabilities of these traditional models. These results reconfirm the
1067 superiority, efficiency and decoupling capability of the proposed model for optimal
1068 allocation cases involving complex water resources system with multiple stakeholders,
1069 multiple sources, multiple decision-makers and embodied reused systems. By
1070 embedding the targets into hierarchical layers, the excessive abandonment of some
1071 promising alternatives is avoided, and optimal allocation is progressively achieved. In
1072 general, the hierarchical structure of the PTSOA model can simulate complicated

1073 systems with multiple complex objectives and constraints.

1074 In addition, the six MOEAs were used to solve the equations in the third layer of
1075 the PTSOA model, and the overall targets in the first layer were determined based on
1076 these solutions. The necessary parameters and hyper-parameters were consistent with
1077 those used in the third layer of the PTSOA model. Additionally, the benefits in the
1078 current case with no optimization calculated based on the actual water supply are given
1079 for comparison. The current situation was categorized as a normal scenario, and other
1080 models were established with the same conditions to facilitate further comparison and
1081 analysis. There were distinct decision alternatives generated by each model, and the
1082 relevant results are listed based on their value ranges. As shown in Table 4, although
1083 NSGA-II and ϵ -MOEA yield slightly higher F2 values than PTSOA and F3 generated
1084 by IBEA ($4.8 \times 10^8 \sim 7.2 \times 10^8$ Chinese Yuan) is higher than obtained with PTSOA,
1085 PTSOA performs better than other models in most cases. The PTSOA model is shown
1086 to be the best model for obtaining comprehensive benefits for the sub-regions in Yiwu
1087 in the normal scenario, demonstrating that the PTSOA model offers advantages
1088 including identifying the best alternatives and achieving greater sub-regional benefits
1089 than the other models. The proposed model yields $1.76 \times 10^9 \sim 15.67 \times 10^9$ Chinese Yuan
1090 total comprehensive benefit improvement and can save approximately $3.2 \times 10^7 \sim$
1091 4.7×10^7 m³ of conventional water compared to the current values. It is also evident that
1092 the proposed model yields the highest *TSI* values, reflecting the improvement achieved
1093 by considering the synergy of the system. In terms of the targets in the first layer, except

1094 MOEA/D, other traditional models fail to retain enough water (water requirements for
1095 living under extreme drought conditions of the next configuration period) in the
1096 reservoirs to meet future basic needs. For MOEA/D, although it generates a slightly
1097 higher total water supply benefit, with a value of $2.81 \times 10^8 \sim 3.12 \times 10^8$, the total water
1098 supply shortage and the total amount of reserved water in the reservoirs are worse than
1099 the amounts obtained with the proposed model. Borg MOEA, as an efficient and robust
1100 many-objective optimization tool, is characterized by its use of auto-adaptive multi-
1101 operator search and other adaptive features (Reed et al., 2013). The *TSI* value of Borg
1102 MOEA is lower than PTSOA. Therefore, in the *TSI* dimension, its performance is
1103 slightly worse than the PTSOA model. However, it is noticed that the Borg MOEA
1104 algorithm could save around one-fifth of the computing time of the model (around 7h).
1105 In the future, it would be interesting to figure out how to couple the Borg MOEA
1106 algorithm with our PTSOA model in a more efficient and synergetic way. In this study,
1107 our main focus is to find the most synergetic solution through optimization in a complex
1108 system. Thus, PTSOA has accomplished superior performance in this respect. It trades
1109 some economic benefits for enhanced water supply reliability and sustainable
1110 development, resulting in a decrease in the water supply from conventional water plants.

1111 The consideration of reclaimed water in the proposed model effectively reduces
1112 the use of traditional water and improves the quality of the water environment by
1113 reducing sewage discharge, and other benefits are also achieved (such as meeting the
1114 quality standards for river water and guaranteeing that the ecological water demand of

1115 inland rivers is met). The results obtained by the PTSOA model may help guide both
 1116 the government and general public. Our proposed model is superior to traditional
 1117 models. It can not only optimize water resource utilization and secure water supplies
 1118 but also enhance the synergy and environmental quality of water systems. Considering
 1119 synergy across various time scales, the proposed model ensures the synergistic
 1120 allocation of water resources at yearly, monthly and daily scales while securing both
 1121 present and future water supplies.

1122 **Table 4** Comparison of the comprehensive benefits of the five objectives (F1, F2, F3,
 1123 F4, and F5) and the *TSI* values in the current situation and obtained using NSGA-II,
 1124 SPEA-II, ϵ -MOEA, IBEA, MOEA/D, Borg MOEA and PTSOA in the normal
 1125 scenario

Comparison	Comprehensive benefits (10^9 Chinese Yuan)					<i>TSI</i>
	F1	F2	F3	F4	F5	
NSGA-II	2.72~2.86	0.91~1.03	2.57~2.60	3.21~3.37	7.38~9.95	-3.13~-2.82
SPEA-II	2.84~2.97	0.93~0.99	2.58~3.15	3.02~3.68	8.22~9.99	-2.39~-2.46
ϵ -MOEA	2.47~2.33	0.85~1.12	2.21~2.32	3.05~3.18	9.23~9.91	-3.41~-3.06
IBEA	2.57~2.88	0.87~0.92	3.05~3.11	3.20~3.32	5.27~8.28	-3.28~-3.11
MOEA/D	2.55~2.90	0.99~1.02	3.15~3.20	3.34~3.36	9.82~10.11	-2.37~-1.54
Borg MOEA	2.95~3.56	0.80~0.98	1.19~2.23	3.11~3.82	12.88~13.90	-2.51~-1.67
Current situation	2.05	0.83	2.49	3.11	9.87	-3.20
PTSOA	2.63~3.03	0.95~0.99	2.39~2.67	3.84~4.11	10.30~11.22	-1.66~-0.89

1126 5. Conclusions

1127 Applying optimal water allocation models to simultaneously enable economic benefits,
 1128 water preferences and environmental demands at different decision levels, time scales

1129 and regions is a challenge. In this study, a new process-based three-layer synergistic
1130 optimal allocation model (PTSOA) was developed and applied to a real and complex
1131 water allocation system. The model was divided into three layers to coordinate conflicts
1132 of interest among decision makers at different levels and time scales. Furthermore, the
1133 allocation of reclaimed water was embedded in the proposed model for synergistic
1134 optimal allocation of both conventional and unconventional water. A synergistic index
1135 based on network analysis was put forward to reduce competitions among different
1136 stakeholders and facilitate the positive effects of stakeholder interactions. A hierarchical
1137 optimal algorithm was designed to solve the PTSOA model.

1138 The proposed model was applied to a typical city in Southeast China with scarce
1139 water resources and developed industry. Achieving the optimal allocation of water
1140 resources in this kind of water-scarcity offers a valuable reference for other counties in
1141 China. The key findings of this study are as follows. Firstly, the results demonstrated
1142 that the PTSOA model achieved synergistic allocation among hierarchical decision-
1143 makers across various time scales and in different regions, yielding the highest *TSI* (-
1144 1.66 to -0.89) among the contrast models. Secondly, with a synergistic approach, a
1145 reasonable amount of conventional water is retained for future use in cases with
1146 potentially high risk, with volumes of $3.95 \times 10^7 \text{ m}^3$, $3.12 \times 10^7 \text{ m}^3$, and $2.43 \times 10^7 \text{ m}^3$
1147 retained in normal, dry and extremely dry scenarios, respectively. Moreover, 7.35×10^7
1148 m^3 , $7.56 \times 10^7 \text{ m}^3$, and $7.37 \times 10^7 \text{ m}^3$ of conventional water can be saved in the three
1149 scenarios. Thirdly, considering both reclaimed water and conventional water in the

1150 optimization process efficiently improves the quality of municipal water, and more than
1151 1272.21 t/year and 48.81 t/year of COD and ammonia nitrogen emissions are mitigated
1152 compared to those in the current situation. Lastly, distinct from previous models, the
1153 proposed optimal model was implemented with the consideration of spatial dimensions,
1154 which are important but often neglected. The results show that spatial allocation yields
1155 an improvement of 4~95% for the comprehensive benefits in different sub-regions
1156 compared to the benefits achieved with traditional models, and the total comprehensive
1157 benefit increases by $1.76 \times 10^9 \sim 15.67 \times 10^9$ Chinese Yuan compared to that in the current
1158 situation.

1159 These results and conclusions provide valuable references for the evaluations of other
1160 complicated water allocation systems. The optimal allocation scheme can be
1161 determined for a complex water resources system upon consideration of stakeholder
1162 synergy and various hierarchical decision levels, time scales and regions. More in-depth
1163 studies of synergistic optimal water allocation are needed in the future.

1164

1165 *Data availability.* The data used to support the findings of this study are available from
1166 the corresponding author upon request.

1167

1168 *Author contributions.* JL and YPX designed all the experiments. JL and WZ collected
1169 and preprocessed the data. JL and WZ conducted all the experiments and analysed the
1170 results. JL wrote the first draft of the manuscript with contributions from SW and SC.

1171 YPX supervised the study and edited the manuscript.

1172

1173 *Competing interests.* The authors declare that they have no conflict of interest.

1174

1175 *Disclaimer.* Publisher's note: Copernicus Publications remains neutral with regard to

1176 jurisdictional claims in published maps and institutional affiliations

1177

1178 *Acknowledgements.* The editors and two reviewers are greatly acknowledged for their

1179 constructive comments to improve the quality of this paper. The Water Resources

1180 Department of Zhejiang Province and the Yiwu City Water Construction Group Co.,

1181 Ltd., are also greatly acknowledged for providing the data regarding the water system

1182 of Yiwu city used in this study.

1183

1184 *Financial support.* This research is funded by the Major Project of Zhejiang Natural

1185 Science Foundation (LZ20E090001) and the Zhejiang Key Research and Development

1186 Plan (2021C03017).

1187

1188 *Review statement.* This paper was edited by Hongkai Gao and reviewed by two

1189 anonymous referees.

1190 **References**

- 1191 Allen, C., Metternicht, G., and Wiedmann, T.: Prioritising SDG targets: assessing
1192 baselines, gaps and interlinkages, *Sustain. Sci.*, 14, 421–438,
1193 <https://doi.org/10.1007/s11625-018-0596-8>, 2019.
- 1194 Arora, S. R. and Gupta, R.: Interactive fuzzy goal programming approach for bilevel
1195 programming problem, *Eur. J. Oper. Res.*, 194, 368–376,
1196 <https://doi.org/10.1016/j.ejor.2007.12.019>, 2009.
- 1197 Avni, N., Eben-Chaime, M., and Oron, G.: Optimizing desalinated sea water blending
1198 with other sources to meet magnesium requirements for potable and irrigation waters,
1199 *Water Res.*, 47, 2164–2176, <https://doi.org/10.1016/j.watres.2013.01.018>, 2013.
- 1200 Baky, I. A.: Interactive TOPSIS algorithms for solving multi-level non-linear multi-
1201 objective decision-making problems, *Appl. Math. Model.*, 38, 1417–1433,
1202 <https://doi.org/10.1016/j.apm.2013.08.016>, 2014.
- 1203 Bali Swain, R. and Ranganathan, S.: Modeling interlinkages between sustainable
1204 development goals using network analysis, *World Dev.*, 138, 105136,
1205 <https://doi.org/10.1016/j.worlddev.2020.105136>, 2021.
- 1206 Ball, S. A., Jaffe, A. J., Crouse-Artus, M. S., Rounsaville, B. J., and O’Malley, S. S.:
1207 Multidimensional subtypes and treatment outcome in first-time DWI offenders,
1208 *Addict. Behav.*, 25, 167–181, [https://doi.org/10.1016/S0306-4603\(99\)00053-2](https://doi.org/10.1016/S0306-4603(99)00053-2), 2000.
- 1209 Bond, R.: Complex networks: Network healing after loss, *Nat. Hum. Behav.*, 1, 1–2,

1210 <https://doi.org/10.1038/s41562-017-0087>, 2017.

1211 Cetintas, S., Si, L., Xin, Y. P., and Hord, C.: and Lecture Notes in Bioinformatics),
1212 228–236 pp., 2010.

1213 Chen, C., Yuan, Y., and Yuan, X.: An Improved NSGA-III Algorithm for Reservoir
1214 Flood Control Operation, *Water Resour. Manag.*, 31, 4469–4483,
1215 <https://doi.org/10.1007/s11269-017-1759-6>, 2017.

1216 Chen, Y., Ma, J., Wang, X., Zhang, X., and Zhou, H.: DE-RSTC: A rational secure
1217 two-party computation protocol based on direction entropy, *Int. J. Intell. Syst.*, 37,
1218 8947–8967, <https://doi.org/10.1002/int.22975>, 2022.

1219 D’Exelle, B., Lecoutere, E., and Van Campenhout, B.: Equity-Efficiency Trade-Offs
1220 in Irrigation Water Sharing: Evidence from a Field Lab in Rural Tanzania, *World
1221 Dev.*, 40, 2537–2551, <https://doi.org/10.1016/j.worlddev.2012.05.026>, 2012.

1222 Dai, C., Qin, X. S., Chen, Y., and Guo, H. C.: Dealing with equality and benefit for
1223 water allocation in a lake watershed: A Gini-coefficient based stochastic optimization
1224 approach, *J. Hydrol.*, 561, 322–334, <https://doi.org/10.1016/j.jhydrol.2018.04.012>,
1225 2018.

1226 Felipe-Lucia, M. R., Soliveres, S., Penone, C., Fischer, M., Ammer, C., Boch, S.,
1227 Boeddinghaus, R. S., Bonkowski, M., Buscot, F., Fiore-Donno, A. M., Frank, K.,
1228 Goldmann, K., Gossner, M. M., Hädzel, N., Jochum, M., Kandeler, E., Klaus, V. H.,
1229 Kleinebecker, T., Leimer, S., Manning, P., Oelmann, Y., Saiz, H., Schall, P., Schloter,
1230 M., Sch öning, I., Schrumpf, M., Solly, E. F., Stempfhuber, B., Weisser, W. W.,

1231 Wilcke, W., Wubet, T., and Allan, E.: Land-use intensity alters networks between
1232 biodiversity, ecosystem functions, and services, *Proc. Natl. Acad. Sci. U. S. A.*, 117,
1233 28140–28149, <https://doi.org/10.1073/pnas.2016210117>, 2020.

1234 Friesen, J., Rodriguez Sinobas, L., Foglia, L., and Ludwig, R.: Environmental and
1235 socio-economic methodologies and solutions towards integrated water resources
1236 management, *Sci. Total Environ.*, 581–582, 906–908,
1237 <https://doi.org/10.1016/j.scitotenv.2016.12.051>, 2017.

1238 Gao, J., Liu, F., Zhang, J., Hu, J., and Cao, Y.: Information entropy as a basic building
1239 block of complexity theory, *Entropy*, 15, 3396–3418,
1240 <https://doi.org/10.3390/e15093396>, 2013.

1241 Haguma, D. and Leconte, R.: Long-Term Planning of Water Systems in the Context
1242 of Climate Non-Stationarity with Deterministic and Stochastic Optimization, *Water*
1243 *Resour. Manag.*, 32, 1725–1739, <https://doi.org/10.1007/s11269-017-1900-6>, 2018.

1244 Han, Y., Xu, S. G., and Xu, X. Z.: Modeling multisource multiuser water resources
1245 allocation, *Water Resour. Manag.*, 22, 911–923, [https://doi.org/10.1007/s11269-007-](https://doi.org/10.1007/s11269-007-9201-0)
1246 [9201-0](https://doi.org/10.1007/s11269-007-9201-0), 2008.

1247 Hu, Z., Wei, C., Yao, L., Li, L., and Li, C.: A multi-objective optimization model
1248 with conditional value-at-risk constraints for water allocation equality, *J. Hydrol.*,
1249 542, 330–342, <https://doi.org/10.1016/j.jhydrol.2016.09.012>, 2016.

1250 Jin, S. W., Li, Y. P., and Nie, S.: An integrated bi-level optimization model for air
1251 quality management of Beijing’s energy system under uncertainty, *J. Hazard. Mater.*,

1252 350, 27–37, <https://doi.org/10.1016/j.jhazmat.2018.02.007>, 2018.

1253 Jinhua ecological Environment Bureau Yiwu branch. Yiwu Ecological City
1254 Construction Plan, 2020.

1255 Li, J., Song, S., Ayantobo, O. O., Wang, H., Jiaping, L., and Zhang, B.: Coordinated
1256 allocation of conventional and unconventional water resources considering
1257 uncertainty and different stakeholders, *J. Hydrol.*, 605, 127293,
1258 <https://doi.org/10.1016/j.jhydrol.2021.127293>, 2022.

1259 Liu, X., Sang, X., Chang, J., Zheng, Y., and Han, Y.: Rainfall prediction optimization
1260 model in ten-day time step based on sliding window mechanism and zero sum game,
1261 *Aqua Water Infrastructure, Ecosyst. Soc.*, 71, 1–18,
1262 <https://doi.org/10.2166/aqua.2021.086>, 2022.

1263 Liu, Y. W., Wang, W., Hu, Y. M., and Liang, Z. M.: Drought assessment and
1264 uncertainty analysis for Dapoling basin, *Nat. Hazards*, 74, 1613–1627,
1265 <https://doi.org/10.1007/s11069-014-1259-4>, 2014.

1266 Pourshahabi, S., Rakhshandehroo, G., Talebbeydokhti, N., Nikoo, M. R., and
1267 Masoumi, F.: Handling uncertainty in optimal design of reservoir water quality
1268 monitoring systems, *Environ. Pollut.*, 266,
1269 <https://doi.org/10.1016/j.envpol.2020.115211>, 2020.

1270 Qiang Yue, Zhang, Y., Li, C., Xue, M., Hou, L., and Wang, T.: Research of Water
1271 Environment Capacity Allocation in Liaoning Province Based on the Analytic
1272 Network Process, *Water Resour.*, 48, 310–323,

1273 <https://doi.org/10.1134/S0097807821020111>, 2021.

1274 Reed, P. M., Hadka, D., Herman, J. D., Kasprzyk, J. R., and Kollat, J. B.:

1275 Evolutionary multiobjective optimization in water resources: The past, present, and

1276 future, *Adv. Water Resour.*, 51, 438–456,

1277 <https://doi.org/10.1016/j.advwatres.2012.01.005>, 2013.

1278 Saavedra, S., Stouffer, D. B., Uzzi, B., and Bascompte, J.: Strong contributors to

1279 network persistence are the most vulnerable to extinction, *Nature*, 478, 233–235,

1280 <https://doi.org/10.1038/nature10433>, 2011.

1281 Safari, N., Zarghami, M., and Szidarovszky, F.: Nash bargaining and leader-follower

1282 models in water allocation: Application to the Zarrinehrud River basin, Iran, *Appl.*

1283 *Math. Model.*, 38, 1959–1968, <https://doi.org/10.1016/j.apm.2013.10.018>, 2014.

1284 Vicuna, S., Dracup, J. A., Lund, J. R., Dale, L. L., and Maurer, E. P.: Basin-scale

1285 water system operations with uncertain future climate conditions: Methodology and

1286 case studies, *Water Resour. Res.*, 46, 1–19, <https://doi.org/10.1029/2009WR007838>,

1287 2010.

1288 Wang, Y., Yin, H., Guo, X., Zhang, W., and Li, Q.: Distributed ANN-based two-

1289 stage stochastic fuzzy possibilistic programming with Bayesian model for irrigation

1290 scheduling management, *J. Hydrol.*, 606, 127435,

1291 <https://doi.org/10.1016/j.jhydrol.2022.127435>, 2022.

1292 Weitz, N., Carlsen, H., Nilsson, M., and Skånberg, K.: Towards systemic and

1293 contextual priority setting for implementing the 2030 agenda, *Sustain. Sci.*, 13, 531–

1294 548, <https://doi.org/10.1007/s11625-017-0470-0>, 2018.

1295 Wu, B., Quan, Q., Yang, S., and Dong, Y.: A social-ecological coupling model for
1296 evaluating the human-water relationship in basins within the Budyko framework, *J.*
1297 *Hydrol.*, 619, 129361, <https://doi.org/10.1016/j.jhydrol.2023.129361>, 2023.

1298 Wu, X., Fu, B., Wang, S., Song, S., Li, Y., Xu, Z., Wei, Y., and Liu, J.: Decoupling of
1299 SDGs followed by re-coupling as sustainable development progresses, *Nat. Sustain.*,
1300 5, 452–459, <https://doi.org/10.1038/s41893-022-00868-x>, 2022.

1301 Xu, J., Lv, C., Yao, L., and Hou, S.: Intergenerational equity based optimal water
1302 allocation for sustainable development: A case study on the upper reaches of Minjiang
1303 River, China, *J. Hydrol.*, 568, 835–848, <https://doi.org/10.1016/j.jhydrol.2018.11.010>,
1304 2019.

1305 Yang, W., Sun, D., and Yang, Z.: A simulation framework for water allocation to
1306 meet the environmental requirements of urban rivers: Model development and a case
1307 study for the Liming River in Daqing City, China, *Environ. Fluid Mech.*, 8, 333–347,
1308 <https://doi.org/10.1007/s10652-008-9093-4>, 2008.

1309 Yao, L., Xu, Z., and Chen, X.: Sustainable water allocation strategies under various
1310 climate scenarios: A case study in China, *J. Hydrol.*, 574, 529–543,
1311 <https://doi.org/10.1016/j.jhydrol.2019.04.055>, 2019.

1312 Yiwu Ecological Environment Status Bulletin, 2020:
1313 https://www.yw.gov.cn/art/2021/10/27/art_1229451977_3928575.html, last access: 27
1314 October 2021.

1315 Jinhua Water Resources Bulletin, 2020: [2326a9df7a784f16b61b42db94b2cf61.pdf](https://doi.org/10.1007/s11269-017-1669-7)
1316 (zj.gov.cn). last access: 2021.

1317 Yu, B., Zhang, C., Jiang, Y., Li, Y., and Zhou, H.: Conjunctive use of Inter-Basin
1318 Transferred and Desalinated Water in a Multi-Source Water Supply System Based on
1319 Cost-Benefit Analysis, *Water Resour. Manag.*, 31, 3313–3328,
1320 <https://doi.org/10.1007/s11269-017-1669-7>, 2017.

1321 Yue, Q., Wang, Y., Liu, L., Niu, J., Guo, P., and Li, P.: Type-2 fuzzy mixed-integer
1322 bi-level programming approach for multi-source multi-user water allocation under
1323 future climate change, *J. Hydrol.*, 591, 125332,
1324 <https://doi.org/10.1016/j.jhydrol.2020.125332>, 2020.

1325 Zhang, K., Yan, H., Zeng, H., Xin, K., and Tao, T.: A practical multi-objective
1326 optimization sectorization method for water distribution network, *Sci. Total Environ.*,
1327 656, 1401–1412, <https://doi.org/10.1016/j.scitotenv.2018.11.273>, 2019a.

1328 Zhang, W., Lei, K., Yang, L., and Lv, X.: Impact of Riverine Pollutants on the Water
1329 Quality of Lake Chaohu, China, *IOP Conf. Ser. Mater. Sci. Eng.*, 484,
1330 <https://doi.org/10.1088/1757-899X/484/1/012049>, 2019b.

1331 Zhang, X. and Vesselinov, V. V.: Energy-water nexus: Balancing the tradeoffs
1332 between two-level decision makers, *Appl. Energy*, 183, 77–87,
1333 <https://doi.org/10.1016/j.apenergy.2016.08.156>, 2016.

1334 Zhao, J., Wu, X., Guo, J., Zhao, H., and Wang, Z.: Study on the Allocation of SO₂
1335 Emission Rights in the Yangtze River Delta City Agglomeration Region of China

- 1336 Based on Efficiency and Feasibility, *Sustain. Cities Soc.*, 87, 104237,
1337 <https://doi.org/10.1016/j.scs.2022.104237>, 2022.
- 1338 Zhou, X. and Moinuddin, M.: Sustainable Development Goals Interlinkages and
1339 Network Analysis: A practical tool for SDG integration and policy coherence, *Inst.*
1340 *Glob. Environ. Strateg.*, 140, 2017.
- 1341 Zivieri, R.: Magnetic Skyrmions as Information Entropy Carriers, *IEEE Trans. Magn.*,
1342 58, 2–6, <https://doi.org/10.1109/TMAG.2021.3092693>, 2022.
- 1343 Zhao, J., 2014. Analysis of the Loss of Water Surface Evaporation and Its Variation
1344 Characteristic in Zhuzhuang Reservoir. *South. Tran.Tech.*12(4).
1345 <https://doi.org/10.13476/j.cnki.nsbdkq.2014.04.048> (In Chinese)